TECHNICAL MEMORANDUM
X-210

INVESTIGATION OF THE SUBSONIC STABILITY AND CONTROL

CHARACTERISTICS OF A 1/7-SCALE MODEL OF THE

NORTH AMERICAN X-15 AIRPLANE WITH AND

WITHOUT FUSELAGE FOREBODY STRAKES

By James L. Hassell, Jr., and Donald E. Hewes

Langley Research Center
Langley Field, Va.

NATIONAL AERONAUTICS AND SPACE ADMINISTRATION

WASHINGTON

February 1960
Declassified May 29, 1960

NATIONAL AERONAUTICS AND SPACE ADMINISTRATION

TECHNICAL MEMORANDUM X-210

INVESTIGATION OF THE SUBSONIC STABILITY AND CONTROL

CHARACTERISTICS OF A 1/7-SCALE MODEL OF THE

NORTH AMERICAN X-15 AIRPLANE WITH AND

WITHOUT FUSELAGE FOREBODY STRAKES

By James L. Hassell, Jr., and Donald E. Hewes

SUMMARY

An investigation of the low-subsonic stability and control charac-
teristics of a 1/7-scale free-flying model modified to represent closely
the North American X-15 airplane (configuration 3) has been made in the
Langley full-scale tunnel. Flight conditions at a relatively low alti-
tude were simulated with the center of gravity at 16.0 percent of the
mean aerodynamic chord.

The longitudinal stability and control were considered to be satis-
factory for all flight conditions tested. The lateral flight behavior
was generally satisfactory for angles of attack below about 20°. At
higher angles, however, the model developed a tendency to fly in a side-
slipped attitude because of static directional instability at small
sideslip angles. Good roll control was maintained to the highest angles
tested, but rudder effectiveness diminished with increasing angle of
attack and became adverse for angles above 40°. Removal of the lower
rudder had little effect on the lateral flight characteristics for angles
of attack less than about 20° but caused the lateral flight behavior to
become worse in the high angle-of-attack range. The addition of small
fuselage forebody strakes improved the static directional stability and
lateral flight behavior of both configurations.

INTRODUCTION

The low-speed stability and control characteristics of a 1/7-scale
free-flying model of the North American X-15 airplane (configuration 1)
were reported in reference 1. (Configuration 1 was the initial design

for which the fuselage side fairings extended to the nose and most of
the vertical-tail area was on top of the fuselage.) The same model used
in the investigation of reference 1 was modified for use in the present
investigation by cutting back the original fuselage side fairings to a
point about 25 percent of the fuselage length from the nose and replacing
the original double-wedge vertical tails with approximately symmetrical
single-wedge vertical tails. The basic fuselage diameter of configura-
tion 1 was not altered when the side fairings were cut back; therefore,
the model used in the present investigation differed from the final
version (configuration 3) of the X-15 airplane in that it had a somewhat
slimmer nose.

In order to determine the effect of these modifications on the low-
speed static stability and control characteristics, force tests were
made of the modified model. In view of the fact that the results of these
tests indicated some marked differences between the static characteristics
of the original and modified models, flight tests of the modified model
were conducted in the Langley full-scale tunnel.

The investigation included a study of the effects of small fuselage
forebody strakes on the directional stability and general flight behavior
of the model. An evaluation was made of the dynamic stability and con-
trol characteristics of both the complete configuration and the configura-
tion with the lower rudder off (to simulate the configuration with the
lower rudder jettisoned for landing).

SYMBOLS

The longitudinal data are referred to the wind system of axes and
the lateral data are referred to the body system of axes. (See fig. 1.)
Unless otherwise specified all data are referred to a center-of-gravity
position of 16.0 percent of the mean aerodynamic chord.

S   wing area, sq ft

$\bar{c}$ wing mean aerodynamic chord, ft

b   wing span, ft

V   airspeed, ft/sec

q   dynamic pressure, $\rho V^2/2$, lb/sq ft

ρ air density, slugs/cu ft

α angle of attack of fuselage reference line, deg

β angle of sideslip, deg

ϕ angle of bank, deg

ψ angle of yaw, deg

μ_b relative density factor, $\dfrac{m}{\rho Sb}$

m mass, slugs

W weight, lb

R Reynolds number

X,Y,Z body system of axes

F_X longitudinal force along X-body axis, lb

F_Y lateral force along Y-body axis, lb

F_Z normal force along Z-body axis, lb

F_L lift force, $-F_Z \cos \alpha + F_X \sin \alpha$, lb

F_D drag force, $-F_X \cos \alpha - F_Z \sin \alpha$, lb

M_X rolling moment about X-body axis, ft-lb

M_Y pitching moment, ft-lb (same for body or wind axes)

M_Z yawing moment about Z-body axis, ft-lb

C_L lift coefficient, F_L/qS

C_D drag coefficient, F_D/qS

C_m pitching-moment coefficient, $M_Y/qS\bar{c}$

C_Y lateral-force coefficient, F_Y/qS

C_l rolling-moment coefficient, M_X/qS

C_n yawing-moment coefficient, M_Z/qSb

$\Delta C_Y, \Delta C_n, \Delta C_l$ incremental force and moment coefficients due to control deflection, effectiveness positive when values are positive

δ_h' deflection of either horizontal tail, positive for trailing edge down, deg

δ_h pitch control deflection, $\dfrac{\delta_{hR}' + \delta_{hL}'}{2}$, deg

δ_a differential roll-control deflection, $\delta_{hR}' - \delta_{hL}'$, deg

δ_r rudder deflection angle, positive for trailing edge left, deg

$$C_{Y_\beta} = \frac{\partial C_Y}{\partial \beta} \text{ per degree} \qquad C_{n_\beta} = \frac{\partial C_n}{\partial \beta} \text{ per degree} \qquad C_{l_\beta} = \frac{\partial C_l}{\partial \beta} \text{ per degree}$$

$$C_{Y_p} = \frac{\partial C_Y}{\partial \frac{pb}{2V}} \qquad C_{n_p} = \frac{\partial C_n}{\partial \frac{pb}{2V}} \qquad C_{l_p} = \frac{\partial C_l}{\partial \frac{pb}{2V}}$$

$$C_{Y_r} = \frac{\partial C_Y}{\partial \frac{rb}{2V}} \qquad C_{n_r} = \frac{\partial C_n}{\partial \frac{rb}{2V}} \qquad C_{l_r} = \frac{\partial C_l}{\partial \frac{rb}{2V}}$$

$$C_{Y_{\dot\beta}} = \frac{\partial C_Y}{\partial \dot\beta} \qquad C_{n_{\dot\beta}} = \frac{\partial C_n}{\partial \dot\beta} \qquad C_{l_{\dot\beta}} = \frac{\partial C_l}{\partial \dot\beta}$$

$$C_{Y_{\delta_a}} = \frac{\partial C_Y}{\partial \delta_a} \text{ per degree} \qquad C_{n_{\delta_a}} = \frac{\partial C_n}{\partial \delta_a} \text{ per degree} \qquad C_{l_{\delta_a}} = \frac{\partial C_l}{\partial \delta_a} \text{ per degree}$$

$$C_{Y_{\delta_r}} = \frac{\partial C_Y}{\partial \delta_r} \text{ per degree} \qquad C_{n_{\delta_r}} = \frac{\partial C_n}{\partial \delta_r} \text{ per degree} \qquad C_{l_{\delta_r}} = \frac{\partial C_l}{\partial \delta_r} \text{ per degree}$$

$$\dot\beta = \frac{d\beta}{dt}$$

k   reduced frequency parameter, $\omega b / 2V$

p   rolling angular velocity, radians/sec

r	yawing angular velocity, radians/sec
ω	angular velocity, radians/sec
I_X, I_Y, I_Z	moment of inertias about X, Y, and Z body axes, slug-ft^2
K_X, K_Y, K_Z	radii of gyration about X, Y, and Z body axes, ft
t	time, sec

Subscripts:

R	right
L	left
F	fuselage
W	wing
H	horizontal tail
V,u	upper vertical tail
R,u	upper rudder
V,l	lower vertical tail
R,l	lower rudder

MODEL AND APPARATUS

The 1/7-scale model used in the investigation was constructed at the Langley Research Center and was the model used in the investigation of reference 1 except for revisions to the fuselage side fairings and vertical-tail arrangement. A three-view drawing of the model is shown in figure 2, and a photograph of the model is shown in figure 3. Table I gives the mass and dimensional characteristics of the final full-scale North American X-15 airplane and the scaled-up mass and dimensional characteristics of the flight-test model used in this investigation.

The model used in the present investigation differed from that used in the investigation of reference 1 in that the original fuselage side fairings were cut back and faired into the fuselage at a point about 25 percent of the fuselage length from the nose. Since the basic fuselage diameter was not altered, the model used in this investigation

differed from the final version of the X-15 airplane in that it had a somewhat slimmer nose. Details of the fuselage-forebody and side-fairing modifications to the flight-test model along with a comparison with the final design are presented in figure 4(a). The double-wedge vertical tails were replaced with approximately symmetrical upper and lower vertical tails having 10° single wedge cross sections. A major portion of both the upper and lower tails was made movable and utilized as rudders.

For some of the tests, small forebody strakes were fitted to the model on both sides of the fuselage at the nose. A sketch showing the strake arrangement used in the investigation is presented in figure 4(b).

For the flight tests, thrust was provided by compressed air supplied through four flexible hoses to four nozzles at the rear of the fuselage. The amount of thrust in the model could be varied and the maximum output per nozzle was about 8 to 10 pounds. The controls were operated by the pilots by means of flicker-type (full on or off) pneumatic servomechanisms which were actuated by electric solenoids. The all-movable horizontal tails were deflected differentially for roll control and together for pitch control. The flicker control deflections used in the flight tests were $\delta_h = \pm 5\frac{1}{2}^{\circ}$, $\delta_r = \pm 7^{\circ}$, and $\delta_a = \pm 16^{\circ}$ ($\pm 8^{\circ}$ of each surface).

Static force tests were made in the Langley free-flight tunnel to determine the static longitudinal and lateral stability and control characteristics of the modified model using the equipment and techniques described in reference 2.

The flight investigation was conducted in the test section of the Langley full-scale tunnel with the test setup illustrated in figure 5. The flight-test equipment is described in detail in reference 1.

DETERMINATION OF STABILITY AND CONTROL PARAMETERS

OF FLIGHT-TEST MODEL

In order to aid in the analysis and interpretation of the flight-test results, the static parameters were determined from static-force-test data and are presented in figures 6 to 16. The static longitudinal parameters were measured over an angle-of-attack range from 0° to 90° at a dynamic pressure of 4.2 pounds per square foot which corresponds to a velocity of about 59 feet per second at the standard sea-level conditions and to a test Reynolds number of about 0.55×10^6 based on the mean aerodynamic chord of 1.47 feet. These tests were made for horizontal-tail deflections of 0°, -10°, -20°, -30° and with horizontal tails off both with and without strakes. Force tests to determine the static

lateral stability characteristics of the model with various tail arrangements were made for an angle-of-attack range from 0° to 60° with angle of sideslip varied from 20° to -20° and at a dynamic pressure of 2.5 pounds per square foot which corresponds to a Reynolds number of about 0.43×10^6. Lateral control characteristics were measured at this same dynamic pressure for an angle-of-attack range from 0° to 70° with horizontal-tail incidence settings from 0° to -30°.

Static Longitudinal Stability and Control

The effect of horizontal-tail deflection on the longitudinal characteristics of the model is shown in figure 6. These data indicate that the model has good static longitudinal stability characteristics (static margin of at least 0.15 for the center of gravity used in this investigation) for all trim lift coefficients up through maximum lift. There is evidence of horizontal-tail surface stalling for the lower tail incidence settings in the region of maximum lift, but the resulting instability is not considered important since it occurs for untrimmed conditions.

Addition of the strakes to the model (fig. 6(b)) caused only minor changes in the static longitudinal characteristics, and for trimmed conditions the strakes caused essentially no change in stability. With the horizontal tails removed, there was a small destabilizing shift in the pitching-moment curve when the strakes were added.

A comparison of the pitching-moment characteristics of the modified 1/7-scale model used in this investigation and an exact 1/10-scale model of the final X-15 configuration (configuration 3) with the horizontal tails on is presented in figure 7. The data which were measured at the same Reynolds number for the two models indicate that the 1/7-scale flight test model is somewhat less stable than the 1/10-scale model of configuration 3. Also shown on the same figure are some unpublished data obtained in an investigation in the Langley 300 MPH 7- by 10-foot wind tunnel which illustrate the effect of increasing Reynolds number on the pitching-moment characteristics of the 1/10-scale model. These results indicate a very pronounced stabilizing effect of increasing Reynolds number up to 1.51×10^6. Because of the differences in fuselage geometry and test Reynolds number, the 1/7-scale free-flight model should have less static longitudinal stability than is anticipated for the full-scale airplane. The model longitudinal flight test results should therefore be considered somewhat conservative.

Static Lateral Stability

The lateral stability data are presented in figure 8 as the variation of the coefficients C_Y, C_n, and C_l with angle of sideslip for angles

of attack up to $40°$. These data are summarized in figure 9 in the form of the side-force parameter C_{Y_β}, the directional stability parameter C_{n_β}, and the effective dihedral parameter C_{l_β} which were obtained by measuring slopes of the linear portion of the curves near zero sideslip. Since some of the data of figure 8 are nonlinear with angle of sideslip, the derivative data shown in figure 9 should only be used as an indication of trends in the data.

Configuration without strakes.- The data of figure 9 show that the complete configuration has a relatively large amount of directional stability at low and high angles of attack but is directionally unstable at intermediate angles. This directional instability exists only for small sideslip angles since there is a nonlinear variation of C_n with β for these angles of attack. (See figs. 8(c), 8(d), and 8(e).) This unusual variation of directional stability will be discussed in more detail in later sections. Removal of the lower rudder caused a relatively small loss of directional stability in the low angle-of-attack range but caused an extremely large loss at the higher angles of attack. (See fig. 9.) The results of figure 9 indicate that the increase in directional stability of the complete configuration in the high angle-of-attack range can be attributed partly to the lower rudder and partly to the wing-fuselage combination. Likewise, these results indicate that the upper vertical tail is highly destabilizing at the higher angles of attack. Apparently, for these high angles, the lower rudder is located in a favorable flow region and the upper vertical tail is in a highly adverse flow region.

Effect of strakes.- Since the directional instability of the complete configuration was associated with a nonlinear variation of C_n with β near zero sideslip (see fig. 8), it was felt that the use of some device on the nose of the model which might favorably affect the flow at small sideslip angles possibly could lead to improved directional stability characteristics. The use of fuselage forebody strakes to produce such flow changes with resulting improvements in directional stability has been suggested in reference 3 and demonstrated in references 4 to 7. Small strakes were therefore fitted to the model used in this investigation as illustrated in figure 4(b) in an effort to improve its directional stability characteristics.

The effect of the addition of these strakes on the variation of the lateral coefficients with sideslip is shown by the data of figure 8. For the complete configuration at angles of attack between $20°$ and $30°$ (figs. 8(c), 8(d), and 8(e)) the variation of C_n with β is nonlinear and directional instability is indicated for small angles of sideslip but, when strakes were added to the configuration, these nonlinearities were largely eliminated so that the variations with sideslip become stable.

The effects of the strakes on the static lateral stability derivatives of the model are shown in figure 9. A comparison of the corresponding curves of figures 9(a) and 9(b) indicates an appreciable improvement in the static directional stability for each of the configurations tested. With the strakes on, in fact, there was no region of directional instability for either the complete configuration or the configuration with the lower rudder off. The effect of strakes on the contribution of the various components of the model to directional stability is shown in figure 10. This figure shows that strakes increase the stability of the wing—fuselage—horizontal-tail combination, increase the contribution of the upper vertical tail at low and moderate angles of attack, and cause a large decrease in the contribution of the lower rudder at high angles of attack.

Large asymmetries at zero sideslip appear in the data for the strakes-off configuration at the higher angles of attack (figs. 8(c) to 8(g)). The effect of the addition of strakes on these asymmetries is best illustrated in figure 11 which shows the variation of the lateral coefficients with angle of attack at zero sideslip. The asymmetric forces and moments at zero sideslip (particularly the yawing moments) are appreciably reduced by the addition of strakes to both sides of the nose. Figure 11 also shows that the addition of a single strake on one side of the nose produced asymmetric forces and moments of even greater magnitude than were experienced on the basic model. With a single strake fitted to the left-hand side of the nose, positive side-force and yawing moments were introduced. This same effect was noted in reference 6 and was attributed to a lower pressure region on the side of the fuselage opposite the strake. The change in sidewash resulting from the change in pressure distribution at the nose also affects the direction of flow in the region of the vertical tails; consequently, the net change in forces and moments cannot be attributed entirely to the pressure change on the nose. For a more detailed interpretation of the effect of strakes on pressure distribution and flow, see references 6 and 7.

Effect of model geometric differences and Reynolds number.- A comparison of the static lateral stability derivatives of a 1/10-scale model of configuration 3 and the 1/7-scale flight test model is presented in figure 12. The data, which were obtained at the same Reynolds number for the two models (0.43×10^6), indicate that the static lateral stability derivatives were generally similar in trend up to an angle of attack of about 20° or 25°. At higher angles of attack the trend toward increasing directional stability for the flight test model was not nearly so pronounced for the 1/10-scale model of configuration 3. The geometric difference (that is, the slimmer nose for the modified model) may have some bearing on the different trends in the lateral characteristics of the two models in the high angle-of-attack range since a change in nose shape can produce flow changes which radically affect the aerodynamic

characteristics. (See refs. 8 and 9.) The fact that the nose strakes had such large effects on static lateral stability characteristics at high angles of attack might be considered another indication of the importance of nose shape.

Also shown in figure 12 are the unpublished lateral data obtained in the Langley 300 MPH 7- by 10-foot wind tunnel which illustrate the effect of increasing Reynolds number on the static lateral stability derivatives of the 1/10-scale model. These data indicate relatively small effects of Reynolds number on C_{n_β} for angles of attack up to about 20° or 25°. At higher angles the variation with increasing Reynolds number is large and inconsistent.

The data of figure 12 show no consistent effect of Reynolds number on effective dihedral ($-C_{l_\beta}$) but do show that the effective dihedral of the 1/7-scale free-flight model was generally more negative than that of the 1/10-scale model of configuration 3 for any Reynolds number.

Static Lateral Control

The roll control effectiveness for several horizontal-tail settings is presented in figure 13. In general, the results obtained for the complete configuration and the lower-rudder-off configuration were similar. The range of effective roll control and favorable yawing moment due to roll control was shifted to higher angles of attack with each increase in negative tail incidence.

The rudder effectiveness for both the complete configuration and the configuration with the lower rudder off is presented in figure 14 for two horizontal-tail incidence settings. These results indicate a gradually decreasing rudder effectiveness with angle of attack. The effects of change in the horizontal-tail incidence on the rudder effectiveness was small. It is interesting to note that removal of the lower rudder resulted in improved rudder effectiveness at angles of attack higher than 35°.

The effective rolling and yawing moment available with coordinated roll control and rudder corresponding to the control deflections used in the flight tests for trim angle-of-attack conditions are presented in figure 15. These data were obtained by interpolating the results of figures 13 and 14 for the proper trim tail incidence in flight corresponding to each trim angle of attack. (It should be noted that trim conditions obtained in the flight tests do not necessarily correspond to the static longitudinal trim data because of thrust and flight cable effects which produce changes in the horizontal-tail incidences required for longitudinal trim.) These results indicate that effective roll control was

maintained for all trim angles of attack tested, but the yawing moments gradually diminished with increasing angle of attack and became adverse at about $\alpha_{trim} = 40^\circ$. The reason for the good roll control over the angle-of-attack range is that the increasing negative tail-incidence settings required for trim with increasing angle of attack tends to keep the horizontal tails unstalled.

FLIGHT TESTS

Flight tests were made to study the dynamic stability and control characteristics of the model using the technique described in reference 1 for a center-of-gravity position of $0.16\bar{c}$ over an angle-of-attack range from 16° to 44°. Both the complete configuration and the configuration without the lower rudder were flight tested with and without the strakes. Combined roll control deflections of $\pm 8^\circ$ of each surface and rudder deflections of $\pm 5^\circ$ were used for all flight conditions. The model was slightly over scaled weight; thus the mass-density ratio of the model ($\mu_b = 46.85$) corresponded to that of the airplane at an altitude of about 8,000 feet.

The model behavior during flight was observed by the pitch pilot located at the side of the test section and by the roll and yaw pilot located in the rear of the test section. The results obtained in the flight tests were primarily in the form of qualitative ratings of flight behavior based on pilot opinion. The motion-picture records obtained in the tests were used to verify and correlate the ratings for the different flight conditions.

FLIGHT-TEST RESULTS AND DISCUSSION

A motion-picture film supplement covering the flight tests has been prepared and is available on loan. A request card form and a description of the film will be found at the back of this paper, on the page immediately preceding the abstract and index page. Table II provides descriptive remarks and numerical data corresponding to each of the flight tests shown in this film supplement. This table is intended primarily as an aid for interpreting this film, but it also serves as a convenient summary of results for the entire flight-test investigation.

Interpretation of Flight-Test Results

It has been shown that the static longitudinal stability of the low Reynolds number, free-flight model is somewhat less than that obtained

on a 1/10-scale model of the final configuration tested at higher
Reynolds numbers, but this difference is of little importance in the
interpretation of these flight-test results since for all test condi-
tions the model had very adequate static longitudinal stability. Also,
it has been shown that for angles of attack up to about 20° the static
directional stability characteristics of the low Reynolds number model
are in good agreement with higher Reynolds number data. Negative
effective dihedral was encountered on the low Reynolds number model at
a lower angle of attack than was indicated by the higher Reynolds number
data. Although flight conditions above an angle of attack of 20° are
not anticipated for the full-scale X-15 airplane during the landing
approach, the model was flight tested to angles of attack as high as
possible. In view of the results obtained from static tests, the model
flight-test results should be applicable to the full-scale flight
behavior of the X-15 airplane for angles of attack up to approximately
20°, but at higher angles of attack the model flight results are not
necessarily representative of anticipated full-scale flight behavior
because of differences in static directional stability characteristics
resulting from differences in fuselage geometry and Reynolds number
effects.

Longitudinal Stability and Control

The longitudinal stability of the model was considered adequate for
all flight conditions tested and there was no noticeable change in the
longitudinal stability characteristics as the angle of attack was
increased from 16° up to 37°. Since the model had a large amount of
static longitudinal stability, the slight loss in static stability
caused by adding the strakes was not noticeable in the flight tests.

The all-movable horizontal tail served as a very powerful pitch
control throughout the angle-of-attack range. Differential deflection
of these surfaces for roll control did not adversely affect the longi-
tudinal characteristics of the model.

Lateral Stability and Control

The flight results pertaining to lateral stability and control were
evaluated for the following four conditions:

(a) Complete configuration without strakes

(b) Complete configuration with strakes

(c) Lower-rudder-off configuration without strakes

(d) Lower-rudder-off configuration with strakes

Complete configuration without strakes.- The lateral stability and control characteristics of the complete configuration without strakes were found to be generally satisfactory up through about an angle of attack of 20°. (See conditions A-1 and A-2 of table II.) As the angle of attack increased above 20°, however, the model had a tendency to fly in a sideslipped attitude either to the right or left. At moderate angles of attack ($\alpha = 23°$, condition A-3) the pilot did not find this flight behavior particularly objectionable, but the tendency for the model to fly in a sideslipped attitude became more pronounced with increasing angle of attack and the model became more difficult to control (conditions A-4 and A-5). At 37° angle of attack (condition A-6) the general flight behavior was unsatisfactory because of poor response to lateral control in addition to the sideslipping condition. The sideslipping flight behavior obtained in these tests was attributed to the asymmetries and nonlinear variations of the lateral coefficients near zero β. There was no evidence of a directional divergence throughout the angle-of-attack range tested. Damping of the lateral oscillation was considered satisfactory for all flight conditions. This damping characteristic is related to the relatively large values of damping-in-roll $\left(C_{l_p} + C_{l_{\dot\beta}} \sin \alpha\right)$ and damping-in-yaw $\left(C_{n_r} - C_{n_{\dot\beta}} \cos \alpha\right)$ parameters shown in figure 16. (Measured values of the rotary oscillation derivatives of the free-flight model from reference 10 are presented here for more convenient correlation with the flight-test results.)

Complete configuration with strakes.- The addition of strakes to the model improved the lateral flight characteristics throughout the angle-of-attack range and especially from 23° to 37° where problems had been encountered with the complete configuration without strakes. At an angle of attack of 21° the general flight behavior of the model was very good. (See condition B-1.) When the angle of attack was increased to 27° (condition B-2), some reduction in directional stability was noted, but the general flight characteristics of the model were still noticeably better than those for the corresponding condition without strakes (condition A-4) because the sideslipping tendency was completely eliminated. When the angle of attack was increased to 31° (condition B-3), the general flight behavior of the model was much better than the corresponding condition without strakes (condition A-5) and also somewhat better than the preceding flight condition (condition B-2). Condition B-3 was, in fact, one of the best flight conditions tested. Both lateral stability and control characteristics were considered very good and an improvement in the directional stability characteristics over the preceding flight condition was indicated. Apparently, this improvement can be attributed to the increased static directional stability in this range. (See fig. 9(b).) Even when the angle of attack was increased to 36°, the general flight behavior was still considered good (condition B-4). The corresponding flight condition without strakes (condition A-6) was judged unsatisfactory because of very pronounced sideslipping and poor response

to lateral control. With strakes installed there was no evidence of any tendency to fly in a sideslipped attitude. Damping of the lateral oscillation was considered satisfactory for all these test conditions. Although the data of figure 16 indicate that the strakes reduced the damping-in-roll and damping-in-yaw parameters in the high angle-of-attack range, no appreciable reduction of damping of the lateral oscillation was noted in the flight tests. When the angle of attack was increased to 44°, the model became very difficult to fly because of a deterioration of lateral control (reduced rolling moment and increased adverse yawing moment). (See condition B-5 and fig. 15.) The general flight behavior for flight condition B-5 was therefore considered unsatisfactory. This problem was apparently one of lateral control rather than of stability, since the data of figures 8 and 9 (for strakes on) indicate even higher levels of static stability for this angle of attack than for lower angles of attack.

Lower-rudder-off configuration without strakes.- When the lower rudder was removed from the basic model without strakes, the lateral stability and control and general flight behavior of the model for angles of attack of 20° or less were considered good and very similar to those of the complete configuration without strakes. (See conditions C-1 and C-2.) With further increase in angle of attack, however, the model was barely flyable (condition C-3, $\alpha = 25°$). The combination of directional instability and negative effective dihedral was apparently the reason for this poor flight behavior. Similar C_{n_β} and C_{l_β} data for the complete configuration at this angle of attack (see fig. 9) resulted in reasonably fair general flight behavior spoiled only by the sideslipping tendency. (See conditions A-3 and A-4.) The primary reason for this difference in the flight characteristics of the complete and lower-rudder-off configurations at an angle of attack of 25° is apparently the difference in the range of sideslip angles over which the directional instability exists. (See data for $\alpha = 25°$ for conditions A and C in table II.) When the angle of attack of the lower-rudder-off configuration was increased further to 29° (condition C-4), the general flight behavior was unsatisfactory. A directional divergence could be prevented only by careful lateral control, and sustained flight could not be maintained for very long periods of time. This configuration could not be flown at higher angles of attack because of increased directional instability.

Lower-rudder-off configuration with strakes.- With the strakes installed the general flight behavior at an angle of attack of 22° was very good (condition D-1) and was noticeably better than the corresponding condition without strakes (condition C-2). When the angle of attack was increased to 25°, a tendency for the model to fly in a sideslipped attitude was noted (condition D-2). This was the first instance of such flight behavior with the strakes installed and also the first noted for the lower-rudder-off configuration. Although this flight behavior was not considered good, it was much better than the corresponding condition

without strakes (condition C-3) for which the model was barely flyable. The data of figure 9 indicate positive C_{n_β} for this condition, but this value of C_{n_β} was measured at zero β. The data of figure 8(d) and table II (condition D-2) show a region of directional instability at small positive angles of sideslip which probably accounts for the side-slipping tendency in this case.

With further increase in angle of attack to 29° the sideslipping tendency became more pronounced (see condition D-3 and fig. 8(e)) and the general flight behavior of the model was considered poor, but this behavior was considered better than that for the corresponding condition without strakes (condition C-4) for which the model was directionally unstable.

Inasmuch as the model with the lower rudder removed could not be flown to as high angles as the complete configuration, the conditions of poor lateral control were not encountered. The lateral damping was considered satisfactory for all flight conditions tested.

SUMMARY OF RESULTS

An investigation of the low-subsonic stability and control characteristics of a 1/7-scale free-flying model modified to represent closely the North American X-15 airplane (configuration 3) has been made in the Langley full-scale tunnel. The results of the investigation may be summarized as follows:

1. Longitudinal stability and control characteristics were satisfactory for all flight conditions tested.

2. The lateral flight behavior was generally satisfactory for angles of attack below about 20°. At higher angles, however, the model developed a tendency to fly in a sideslipped attitude because of static directional instability at small sideslip angles. Good roll control was maintained to the highest angles of attack flown, but yaw control diminished with increasing angle of attack and became adverse at angles above 40°.

3. Removal of the lower rudder had little or no effect on the lateral flight characteristics for angles of attack below about 20° but caused the lateral flight behavior to become worse in the high angle-of-attack range.

4. The addition of small fuselage forebody strakes improved the static directional stability and lateral flight behavior of both configurations in the high angle-of-attack range.

Langley Research Center,
     National Aeronautics and Space Administration,
          Langley Field, Va., September 23, 1959.

REFERENCES

1. Boisseau, Peter C.: Investigation of the Low-Speed Stability and Control Characteristics of a 1/7-Scale Model of the North American X-15 Airplane. NACA RM L57D09, 1957.

2. Hewes, Donald E.: Low-Subsonic Measurements of the Static and Oscillatory Lateral Stability Derivatives of a Sweptback-Wing Airplane Configuration at Angles of Attack From -10° to 90°. NASA MEMO 5-20-59L, 1959.

3. Klinar, Walter J.: A Study by Means of a Dynamic-Model Investigation of the Use of Canard Surfaces as an Aid in Recovering From Spins and as a Means for Preventing Directional Divergence Near the Stall. NACA RM L56B23, 1956.

4. Paulson, John W., and Boisseau, Peter C.: Low-Speed Investigation of the Effect of Small Canard Surfaces on the Directional Stability of a Sweptback-Wing Fighter-Airplane Model. NACA RM L56F19a, 1956.

5. Sleeman, William C., Jr.: Investigation at High Subsonic Speeds of the Effects of Various Horizontal Fuselage Forebody Fins on the Directional and Longitudinal Stability of a Complete Model Having a 45° Sweptback Wing. NACA RM L56J25, 1957.

6. Polhamus, Edward C., and Spreeman, Kenneth P.: Effect at High Subsonic Speeds of Fuselage Forebody Strakes on the Static Stability and Vertical-Tail-Load Characteristics of a Complete Model Having a Delta Wing. NACA RM L57K15a, 1958.

7. Driver, Cornelius: Wind-Tunnel Investigation at a Mach Number of 2.01 of Forebody Strakes for Improving Directional Stability of Supersonic Aircraft. NACA RM L58C11, 1958.

8. Letko, William: A Low-Speed Experimental Study of the Directional Characteristics of a Sharp-Nosed Fuselage Through a Large Angle-of-Attack Range at Zero Angle of Sideslip. NACA TN 2911, 1953.

9. Boisseau, Peter C.: Low-Subsonic Static Stability and Damping Derivatives at Angles of Attack From 0° to 90° for a Model With a Low-Aspect-Ratio Unswept Wing and Two Different Fuselage Forebodies. NASA MEMO 1-22-59L, 1959.

10. Paulson, John W., and Hassell, James L., Jr.: Low-Speed Measurements of Oscillatory Lateral Stability Derivatives of a 1/7-Scale Model of the North American X-15 Airplane. NASA TM X-144, 1959.

TABLE I.- MASS AND GEOMETRIC CHARACTERISTICS OF THE NORTH AMERICAN X-15 AIRPLANE

AND SCALED-UP CHARACTERISTICS OF THE 1/7-SCALE MODEL

[All values for complete configuration with lower rudder on]

	Scaled-up model values (Flight-test model)	North American full-scale (Configuration 3)
Weight (landing approach condition), lb	16,000	12,546
Relative density factor, μ_b	46.85	46.85 (at 8,000 ft)
Wing loading, W/S, lb/sq ft	80.0	62.7
Center-of-gravity position, percent $\bar{c}$	16.0	16.0
Moments of inertia, slug-ft²:		
I_X	8,490	3,378
I_Y	61,100	73,726
I_Z	64,050	75,246
Radii of gyration, ft:		
K_X	4.13	2.95
K_Y	11.08	13.77
K_Z	11.34	13.91
Wing:		
Airfoil section	NACA 66-005 (modified)	NACA 66-005 (modified)
Area, S, sq ft	200	200
Span, b, ft	22.36	22.36
Root chord, ft	14.91	14.91
Tip chord, ft	2.98	2.98
Mean geometric chord, $\bar{c}$, ft	10.27	10.27
Fuselage station of $0.25\bar{c}$	345.86	345.353
Leading-edge sweep, deg	36.75	36.75
Trailing-edge sweep, deg	-17.75	-17.75
Dihedral, deg	0	0
Incidence, deg	0	0
Aspect ratio, b^2/S	2.50	2.50
Taper ratio	0.20	0.20
Fuselage:		
Length (high-speed nose), ft	------	49.17
Length (low-speed nose), ft	49.00	49.83
Extension of high-speed nose forward of fuselage station 0.000, ft	------	0.17
Extension of low-speed nose forward of fuselage station 0.000, ft	------	0.83
Depth (maximum) basic fuselage, ft	4.42	4.67
Width (maximum) including side fairing, ft	7.58	7.33
Horizontal tail:		
Airfoil section (parallel to center line)	NACA 66-005 (modified)	NACA 66-005 (modified)
Area:		
Total (through fuselage), sq ft	110.69	115.34
Exposed (movable), sq ft	50.62	52.05
Span:		
Total (through fuselage), ft	17.63	18.08
Exposed (one surface), ft	5.27	5.50
Root chord, ft	10.02	10.22
Tip chord, ft	2.15	2.17
Fuselage chord, ft	6.95	7.02
Mean geometric chord, $\bar{c}_H$, (based on total area), ft	6.92	7.05
Mean geometric chord, $\bar{c}_{H_{exposed}}$, (based on exposed area), ft	4.96	5.00
Fuselage station of $0.25\bar{c}_H$	494.04	497.663
Fuselage station of $0.25\bar{c}_{H_{exposed}}$	524.00	526.000
Leading-edge sweep, deg	50.58	50.58
Trailing-edge sweep, deg	19.28	19.28
Dihedral, deg	-15.00	-15.00
Aspect ratio (based on total area)	2.82	2.83
Taper ratio	0.21	0.21
Longitudinal distance from $0.25\bar{c}$ to $0.25\bar{c}_{H_{exposed}}$, ft	14.84	15.05

TABLE I.- MASS AND GEOMETRIC CHARACTERISTICS OF THE NORTH AMERICAN X-15 AIRPLANE

AND SCALED-UP CHARACTERISTICS OF THE 1/7-SCALE MODEL - Concluded

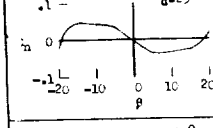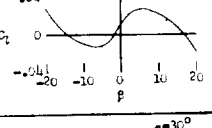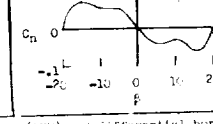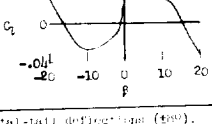|	Scaled-up model values (Flight-test model)	North American full-scale (Configuration 3)
Upper vertical tail:		
Airfoil section	10° wedge	10° wedge
Area:		
Total (above fuselage chord line), sq ft	40.83	40.83
Movable portion, sq ft	26.65	26.65
Span:		
Total (above fuselage chord line), ft	4.69	4.69
Movable portion, ft	3.16	3.16
Fuselage chord, ft	10.16	10.16
Rudder root chord, ft	9.36	9.36
Tip chord, ft	7.53	7.53
Mean geometric chord, $\bar{c}_{V,u}$ (based on total area above fuselage chord line), ft	9.23	9.23
Mean geometric chord, $\bar{c}_{R,u}$ (based on movable area), ft	8.72	8.50
Fuselage station of $0.25\bar{c}_{V,u}$	493.44	493.442
Fuselage station of $0.25\bar{c}_{R,u}$	497.53	497.533
Leading-edge sweep, deg	30.0	30.0
Trailing-edge sweep, deg	0	0
Aspect ratio (based on total area above fuselage chord line) . .	0.52	0.52
Taper ratio	0.74	0.74
Longitudinal distance from $0.25\bar{c}$ to $0.25\bar{c}_{V,u}$, ft	12.30	12.34
Lower vertical tail:		
Airfoil section	10° wedge	10° wedge
Area:		
Total (below fuselage chord line), sq ft	34.48	34.22
Movable (jettisonable) portion, sq ft	20.30	19.95
Span:		
Total (below fuselage chord line), ft	3.82	3.83
Movable (jettisonable) portion, ft	2.33	2.38
Fuselage chord, ft	10.21	10.21
Rudder root chord, ft	9.37	9.48
Tip chord, ft	8.10	7.99
Mean geometric chord, $\bar{c}_{V,l}$ (based on total area below fuselage chord line), ft	9.20	9.17
Mean geometric chord, $\bar{c}_{R,l}$ (based on movable or jettisonable area), ft	8.75	8.72
Fuselage station of $0.25\bar{c}_{V,l}$	491.48	491.483
Fuselage station of $0.25\bar{c}_{R,l}$	497.25	497.250
Leading-edge sweep, deg	30.0	30.0
Trailing-edge sweep, deg	0	0
Aspect ratio (based on total area below fuselage chord line) . .	0.43	0.43
Taper ratio	0.78	0.78
Longitudinal distance from $0.25\bar{c}$ to $0.25\bar{c}_{V,l}$, ft	12.12	12.18

TABLE II.- COMPARISON OF THE LATERAL FLIGHT CHARACTERISTICS WITH THE STATIC

DATA FOR A MODIFIED 1/7-SCALE MODEL OF THE X-15 AIRPLANE

Condition	α_{trim}, deg	Control moment coefficients[1]		Flight test remarks	Variation of C_n with β	Variation of C_l with β
		ΔC_l (combined)	ΔC_n (combined)			
A-1	16	0.023	0.041	General flight behavior is very good.		
A-2	20	.024	.036	General flight behavior is good.		
A-3	23	.025	.030	The model flies at small angles of sideslip but is easy to control. General flight behavior is fair.		
A-4	28	.026	.020	The model has a more pronounced tendency to fly sideslipped on either side of $\beta = 0°$ but is still easy to control. General flight behavior is worse than the previous condition.		
A-5	32	.026	.012	The model flies at large sideslip angles on either side of $\beta = 0°$ and is more difficult to control. General flight behavior is very poor.		
A-6	37	.023	.007	The model flies in a pronounced sideslipped attitude and has very poor response to lateral control; unsatisfactory general flight behavior resulted.		

(a) Complete configuration; strakes off

[1]The control moment coefficients are the total values obtained from combined rudder (±7°) and differential horizontal-tail deflections (±6°).
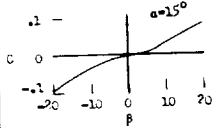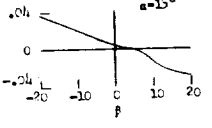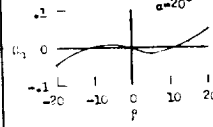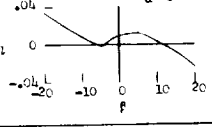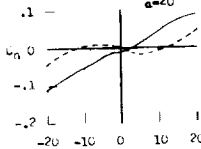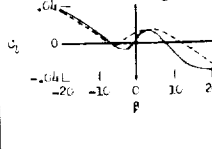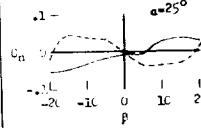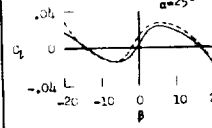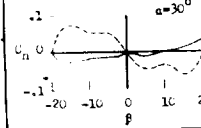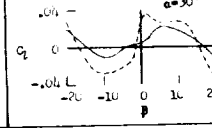
TABLE II.- COMPARISON OF THE LATERAL FLIGHT CHARACTERISTICS WITH THE STATIC

DATA FOR A MODIFIED 1/7-SCALE MODEL OF THE X-15 AIRPLANE - Continued

(b) Complete configuration; strakes on

Condition	α_{trim}, deg	Control moment coefficients[1]		Flight test remarks	Variation of C_n with β	Variation of C_l with β
		ΔC_l (combined)	ΔC_n (combined)			
B-1	21	0.024	0.034	The general flight behavior is very good.	$\alpha=20°$	$\alpha=20°$
B-2	27	.026	.022	The general flight behavior is better than the corresponding condition without strakes (A-4), but not as good as the preceding condition with strakes (B-1).	$\alpha=25°$	$\alpha=25°$
B-3	31	.026	.014	The general flight behavior is much better than the corresponding condition without strakes (A-5) and also somewhat better than the preceding condition with strakes (B-2).	$\alpha=30°$	$\alpha=30°$
B-4	36	.024	.008	The general flight behavior is still good and very similar to the preceding condition (B-3).	$\alpha=35°$	$\alpha=35°$
B-5	44	.016	-.016 (adverse)	The model is difficult to fly because of the reduced rolling moment and adverse yawing moment produced by the combined lateral controls. The general flight behavior is not satisfactory.	$\alpha=40°$ / $\alpha=50°$	$\alpha=40°$ / $\alpha=50°$

[1]The control moment coefficients are the total values obtained from combined rudder (±7°) and differential horizontal-tail deflections (±6°).

——————— Strakes on

- - - - - - - - - - Strakes off

22

TABLE II.- COMPARISON OF THE LATERAL FLIGHT CHARACTERISTICS WITH THE STATIC

DATA FOR A MODIFIED 1/7-SCALE MODEL OF THE X-15 AIRPLANE - Concluded

(c) Lower rudder off; strakes off

Condition	α_{trim}, deg	Control moment coefficients[1] ΔC_l (combined)	ΔC_n (combined)	Flight test remarks	Variation of C_n with β	Variation of C_l with β
C-1	16	0.020	0.040	The general flight behavior is very good.		
C-2	20	.023	.035	The general flight behavior is good (similar to the corresponding condition, A-2, with the lower rudder on).		
C-3	25	.025	.029	The model is barely flyable, apparently because of negative static directional stability and effective dihedral. The general flight behavior is poor.		
C-4	29	.025	.020	Although the model was directionally unstable, a directional divergence could be prevented by careful lateral control. The general flight behavior was unsatisfactory.		

[1]The control moment coefficients are the total values obtained from combined rudder (±7°) and differential horizontal-tail deflections (±8°).

(d) Lower rudder off; strakes on

Condition	α_{trim}, deg	Control moment coefficients[1] ΔC_l (combined)	ΔC_n (combined)	Flight test remarks	Variation of C_n with β	Variation of C_l with β
D-1	22	0.024	0.052	The general flight behavior is very good.		
D-2	25	.025	.029	Although the model has a tendency to fly sideslipped, the general flight behavior is much better than the corresponding condition without strakes (C-3).		
D-3	29	.025	.020	The model has a pronounced tendency to fly sideslipped on either side of $\beta = 0°$. The general flight behavior is poor, but better than the corresponding condition without strakes (C-4).		

[1]The control moment coefficients are the total values obtained from combined rudder (±7°) and differential horizontal-tail deflections (±8°).

Key for d-series conditions only.
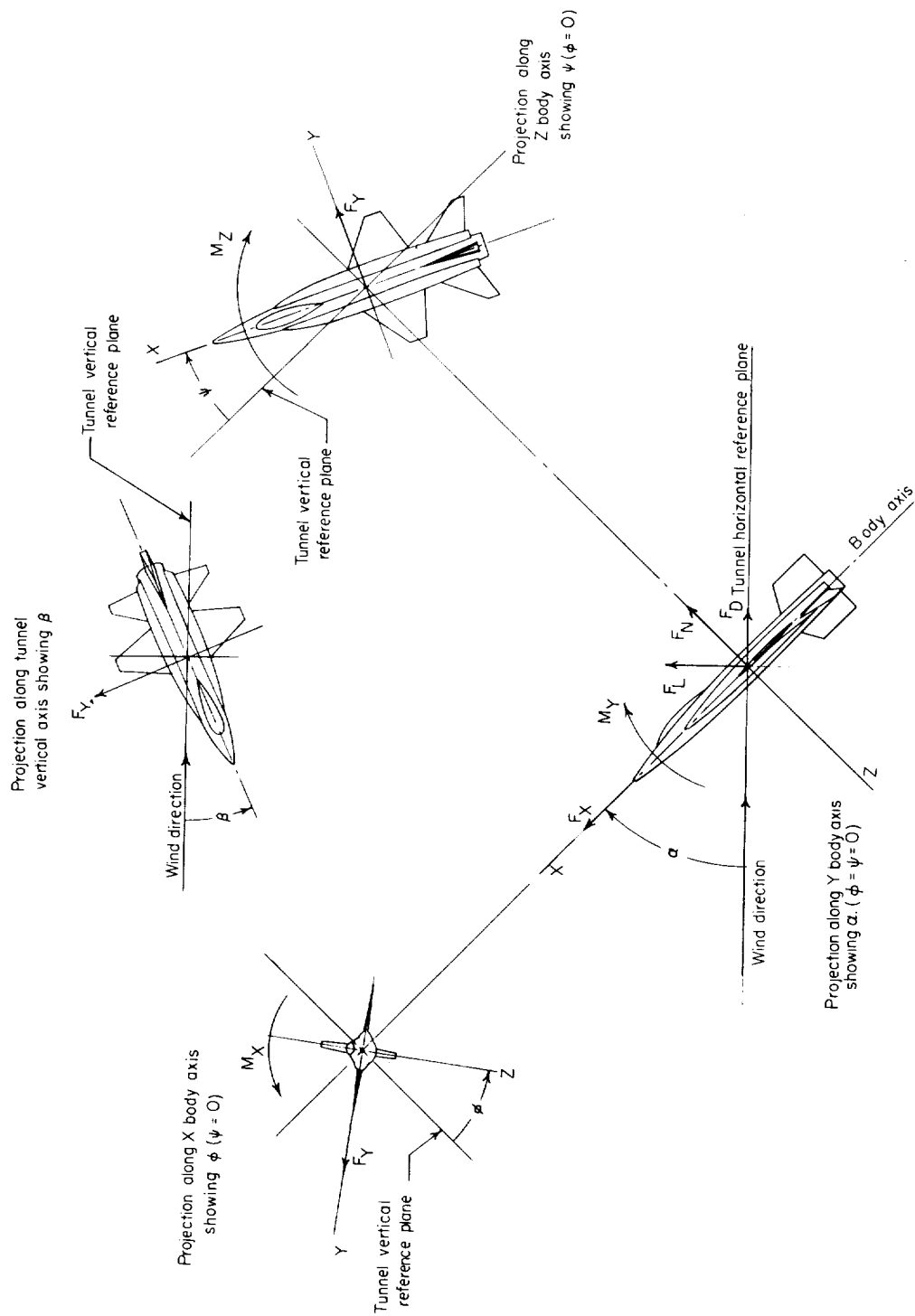——————— Strakes on
- - - - - - - - - Strakes off

Figure 1.- System of axes used in investigation. Longitudinal data are referred to wind system of axes, and lateral data are referred to body system of axes. Arrows indicate positive directions of moments, forces, and angles.
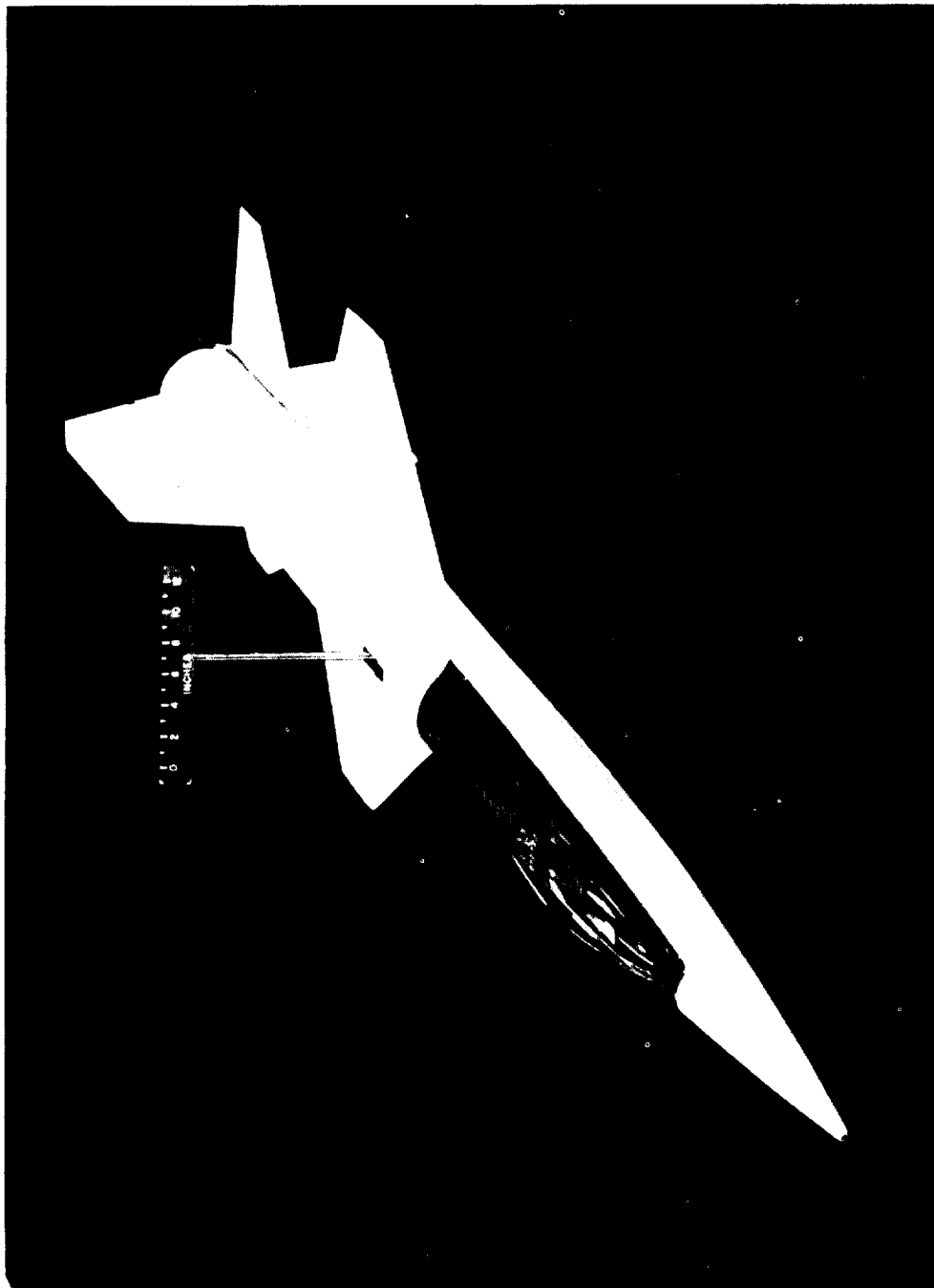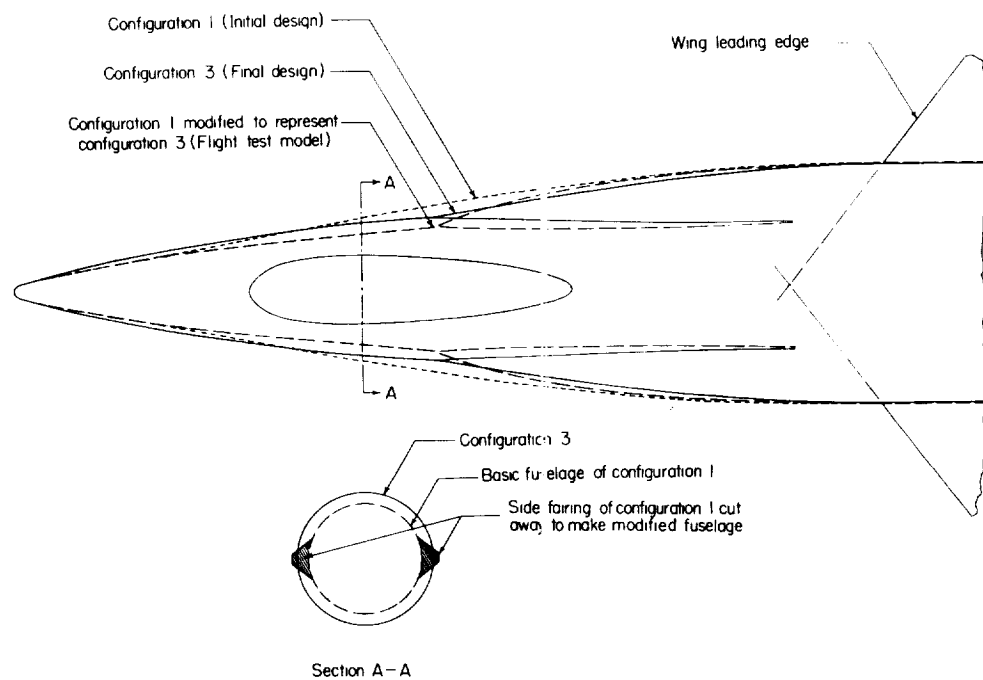
Figure 2.- Three-view drawing of 1/7-scale flight-test model of North
American X-15 airplane used in investigation. All dimensions are in
inches.

Figure 3.- Photograph of model used in investigation.   L-57-5546

Configuration I (Initial design)

Configuration 3 (Final design)

Configuration I modified to represent
configuration 3 (Flight test model)

Wing leading edge

A

A

Configuration 3

Basic fuselage of configuration I

Side fairing of configuration I cut
away to make modified fuselage

Section A—A

(a) Detail of fuselage forebody modification on 1/7-scale
flight-test model as compared with final design.

$10\frac{1}{2}$"

$\frac{1}{4}$" max

A

A

$\frac{1}{16}$"

Section A—A
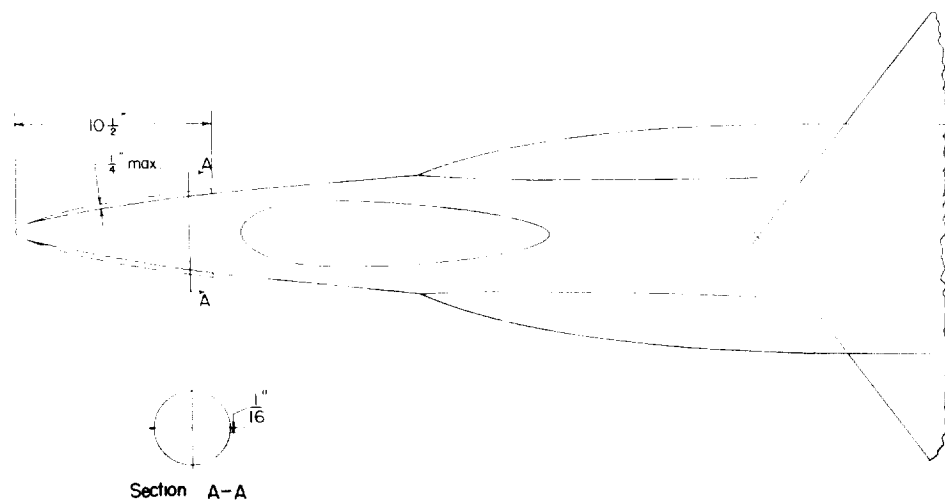
(b) Fuselage forebody strake installation used on 1/7-scale
flight-test model (configuration 1 modified).

Figure 4.- Fuselage forebody side fairing modification and strake
installation.
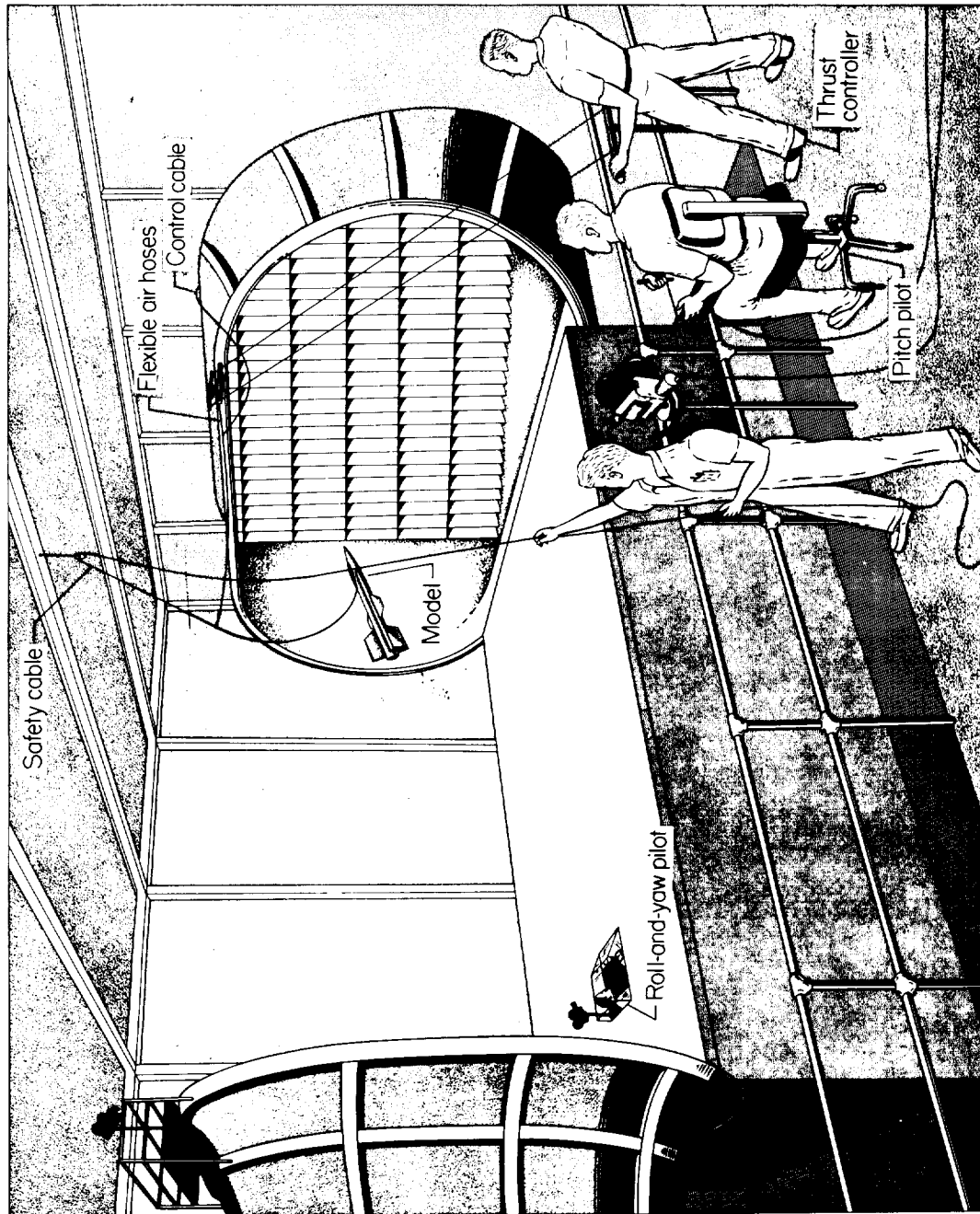
Figure 5.- Sketch of test setup in Langley full-scale tunnel.
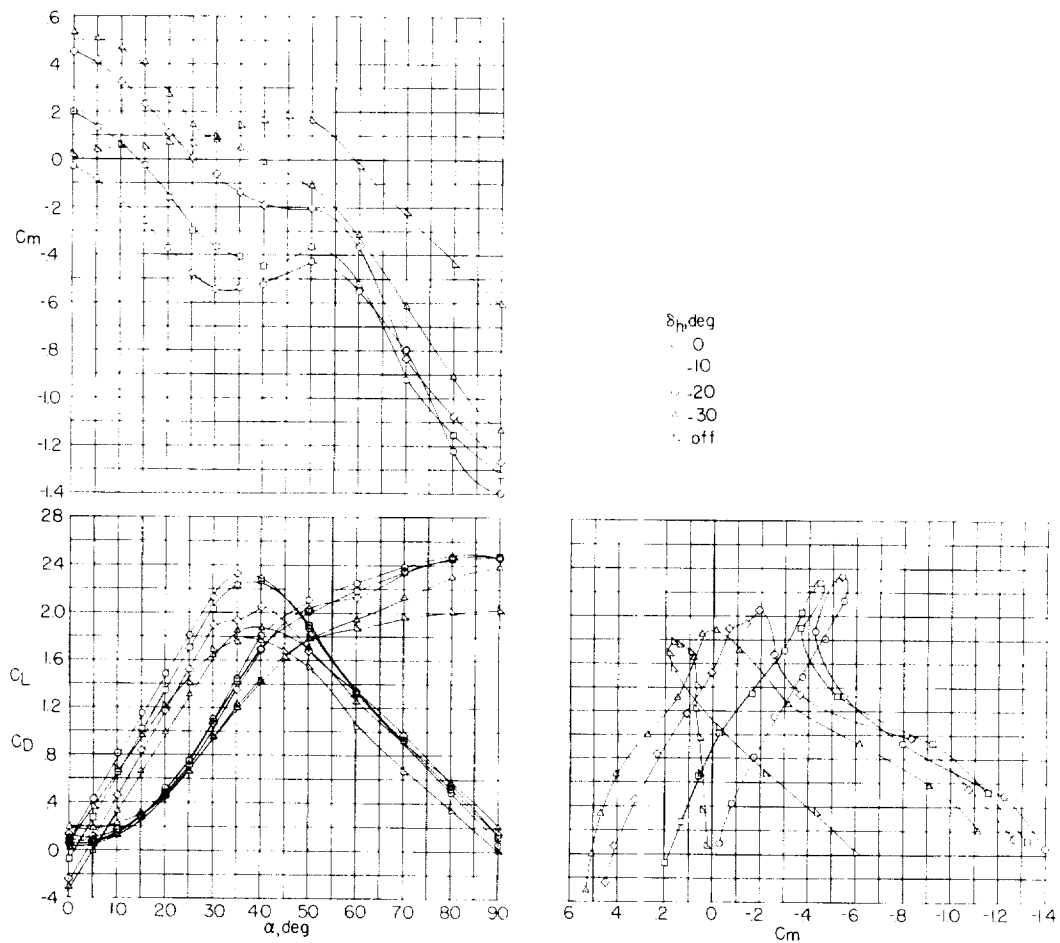
(a) Strakes off.

Figure 6.- Longitudinal characteristics of 1/7-scale flight-test model. Center of gravity at 0.15$\bar{c}$; β = 0°.
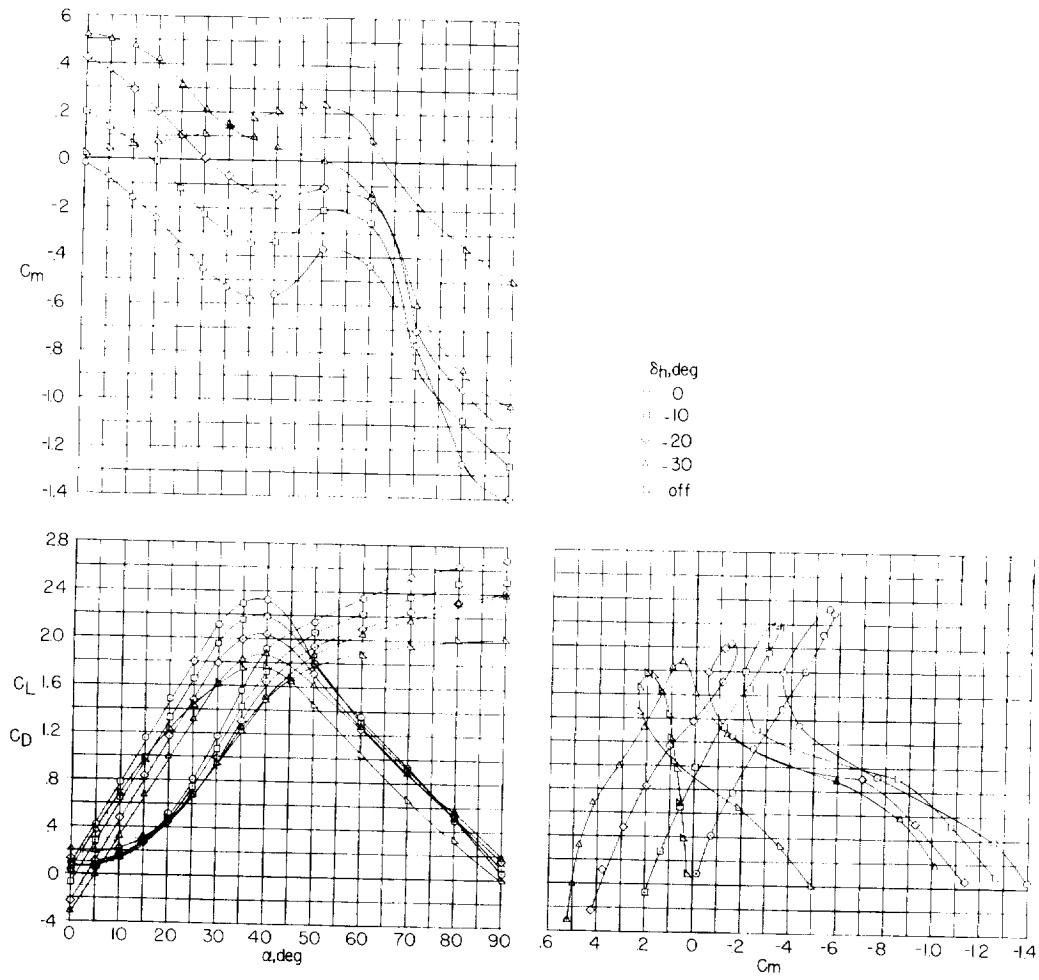
(b) Strakes on.

Figure 6.- Concluded.

	R	Model scal	Configuration number	Source
O	0.55x10⁶	$\frac{1}{7}$	I (modified)	Present paper
□	.55x10⁶	$\frac{1}{10}$	3	
◇	.75x10⁶	$\frac{1}{10}$	3	
△	1.07x10⁶	$\frac{1}{10}$	3	Unpublished data
◺	1.51x10⁶	$\frac{1}{10}$	3	
◹	1.95x10⁶	$\frac{1}{10}$	3	
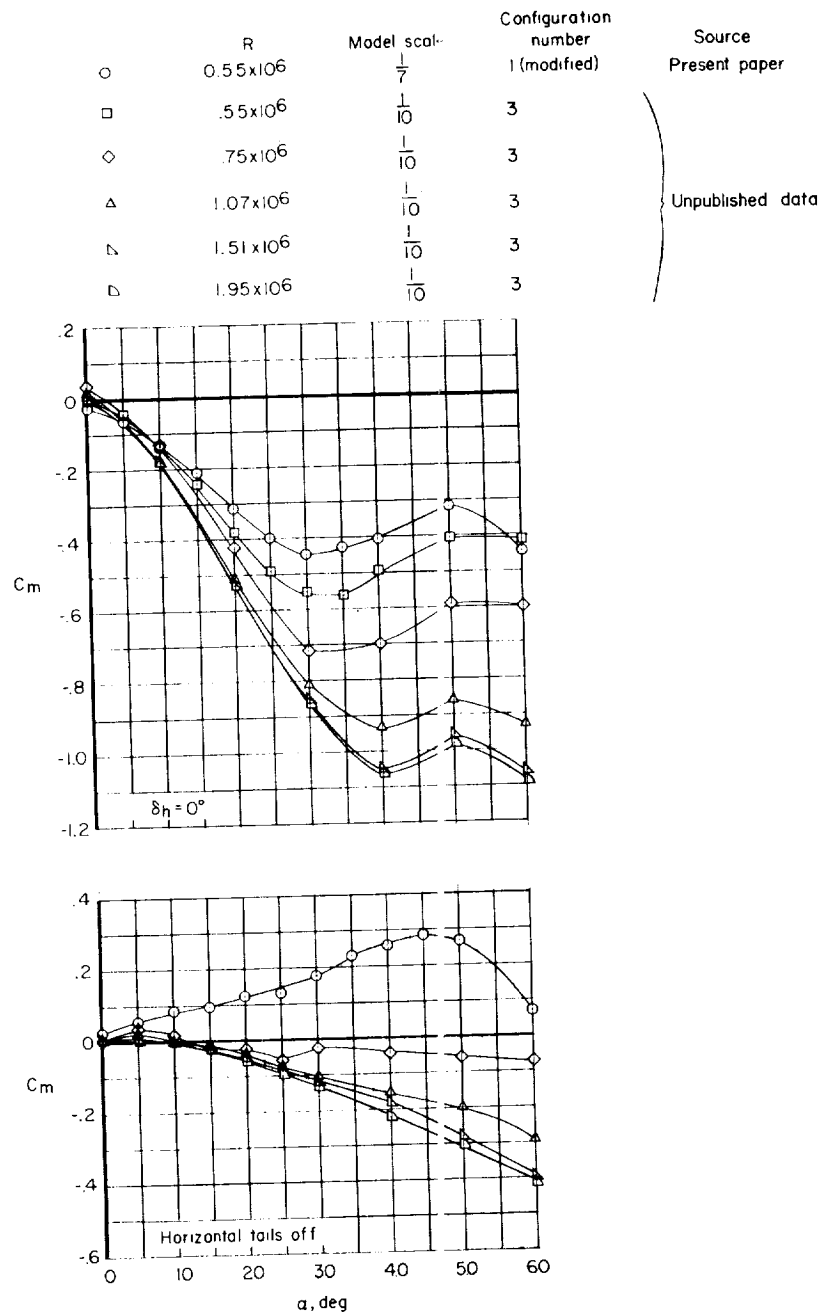
Figure 7.- Effect of model geometry and Reynolds number on variation of pitching-moment coefficient with angle of attack. (1/7-scale model, flight-test configuration; 1/10-scale model, configuration 3.) Center of gravity at 0.20$\bar{c}$; $\beta = 0°$.
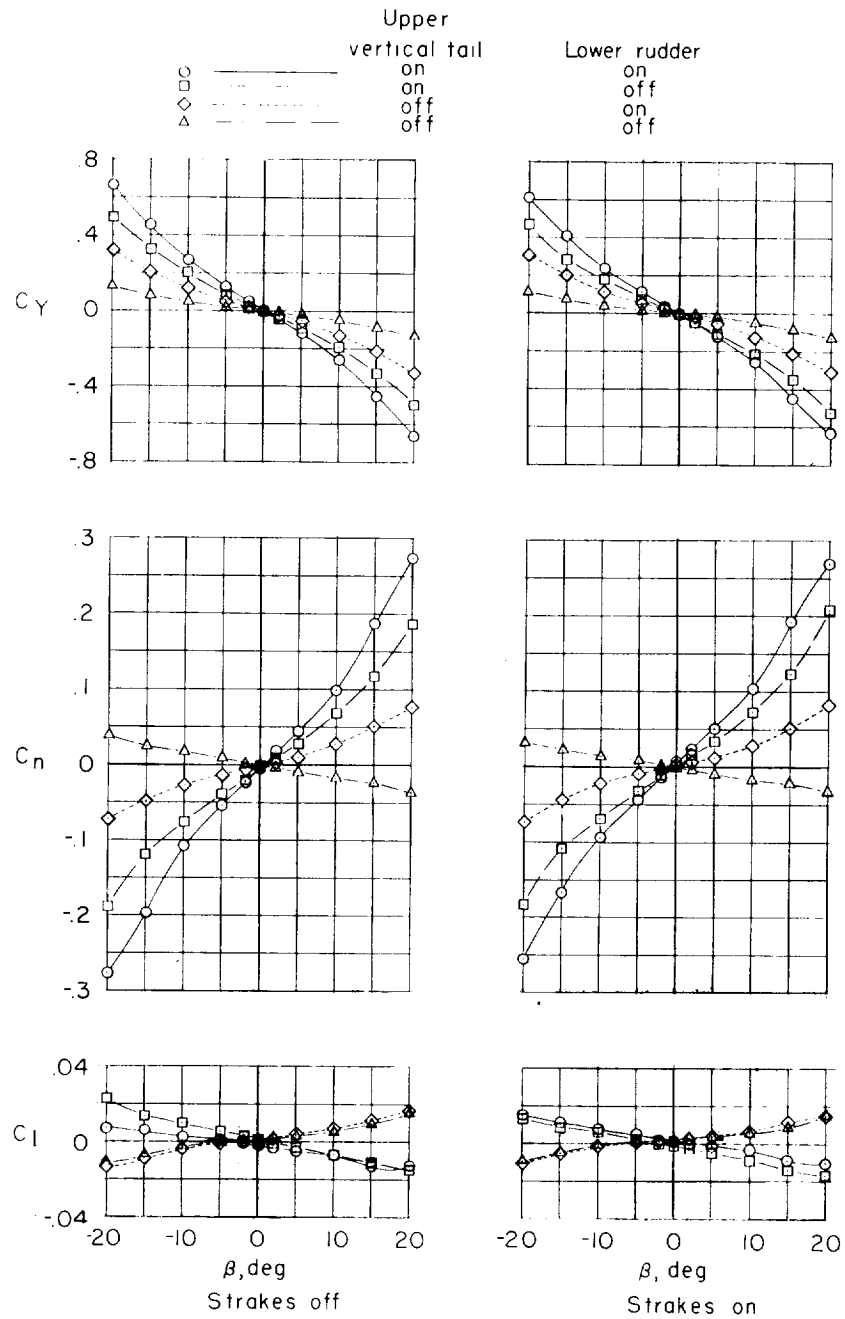
(a) $\alpha = 0°$.

Figure 8.- Variation of static lateral coefficients with angle of side-slip for 1/7-scale flight-test model. $\delta_h = 0°$.
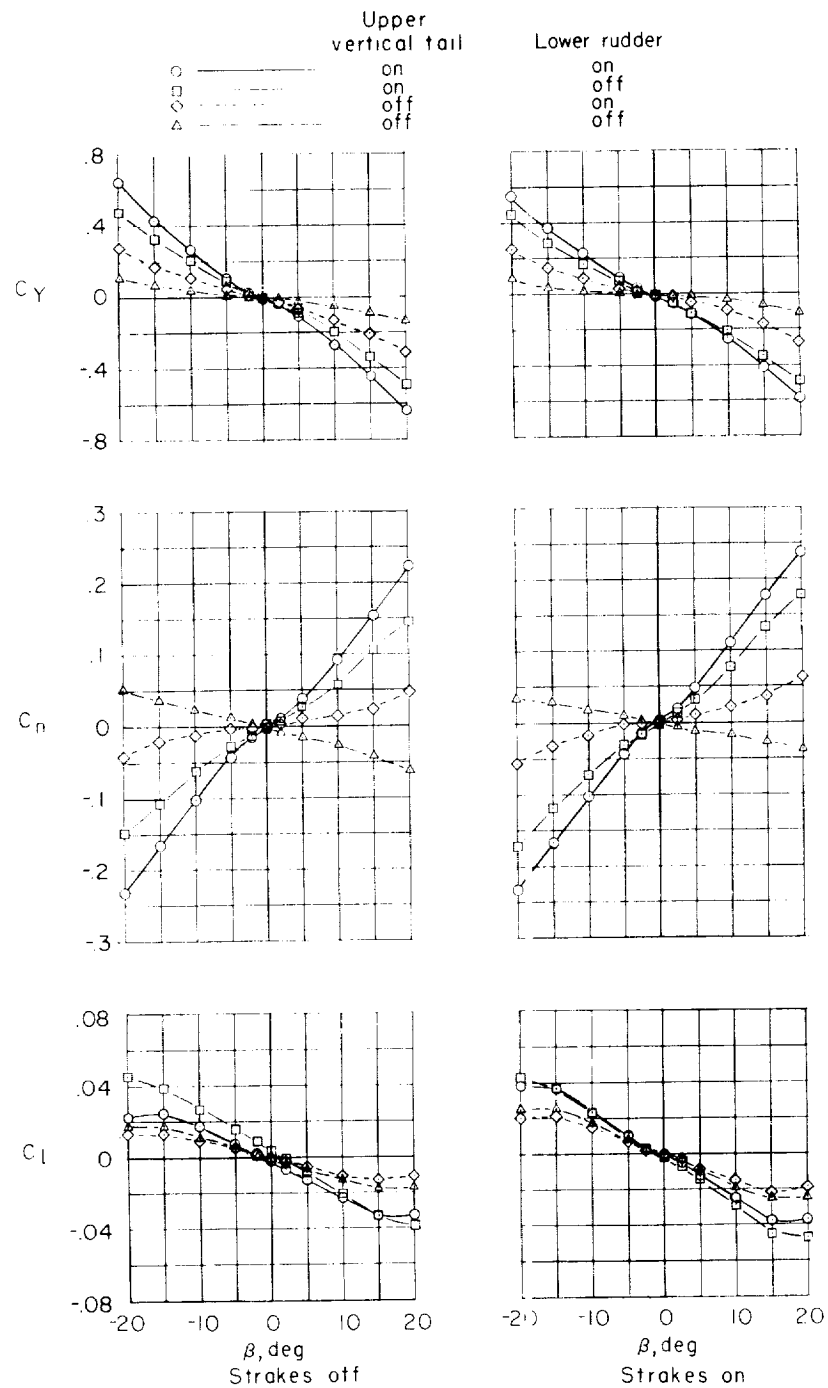
(b) α = 10°.

Figure 8.- Continued.
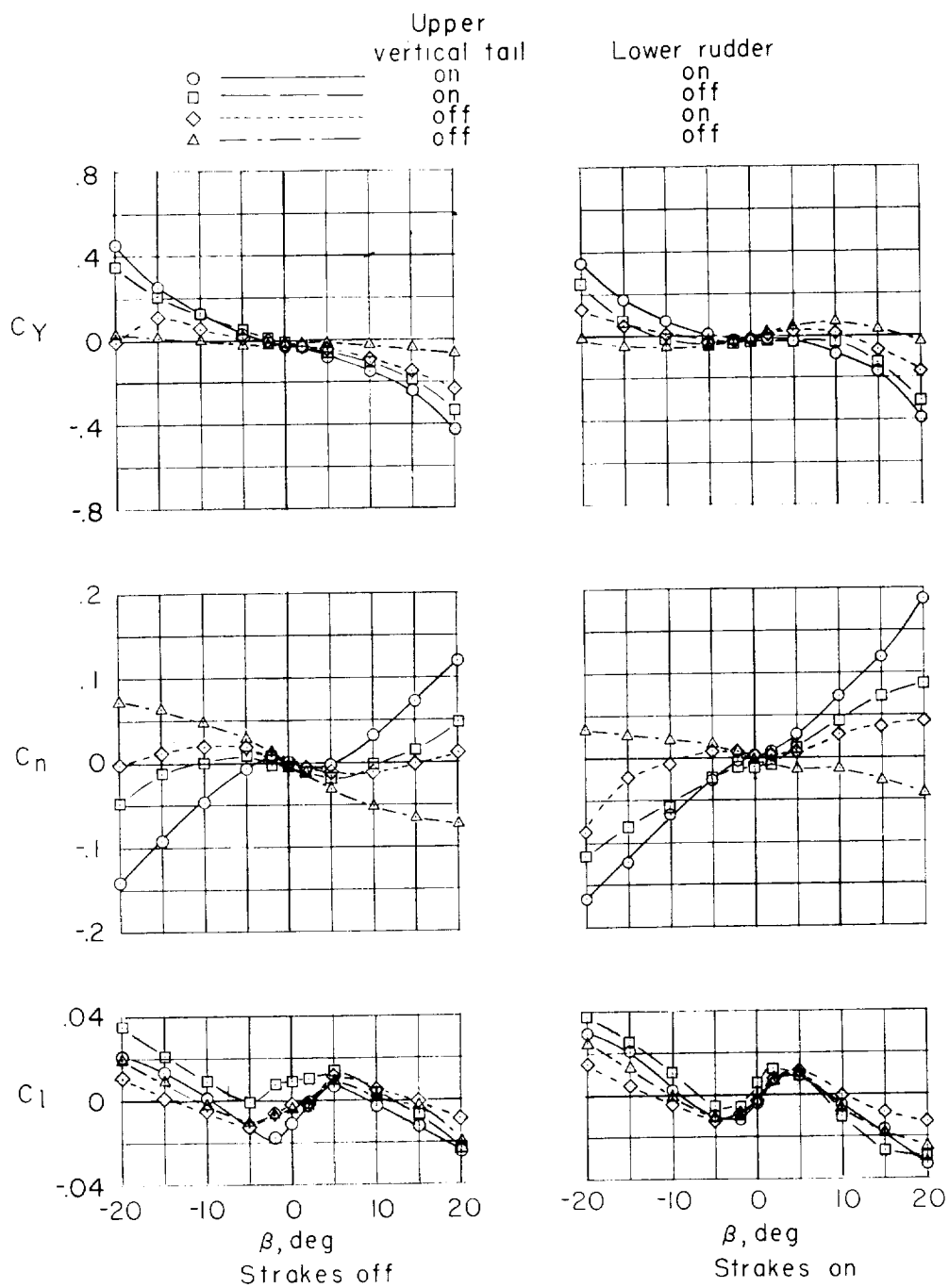
(c) α = 20°.

Figure 8.- Continued.

(d) α = 25°.

Figure 8.- Continued.

(e) α = 30°.

Figure 8.- Continued.

Upper
vertical tail
Lower rudder

(f) α = 35°.

Figure 8.- Continued.

Upper
vertical tail   Lower rudder
○ ————————   on   on
□ — — — —   on   off
◇ ....   off   on
△ —·—·—   off   off
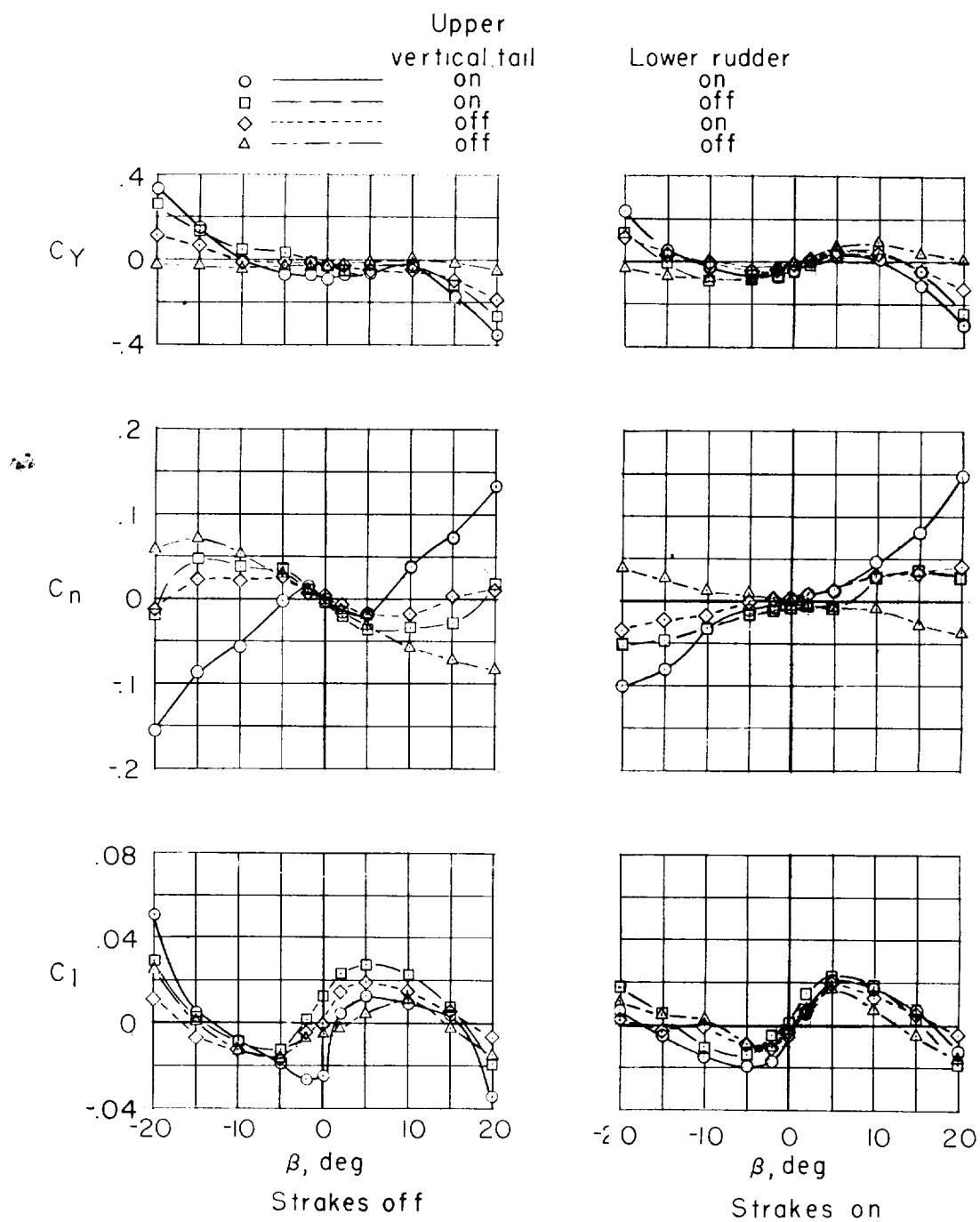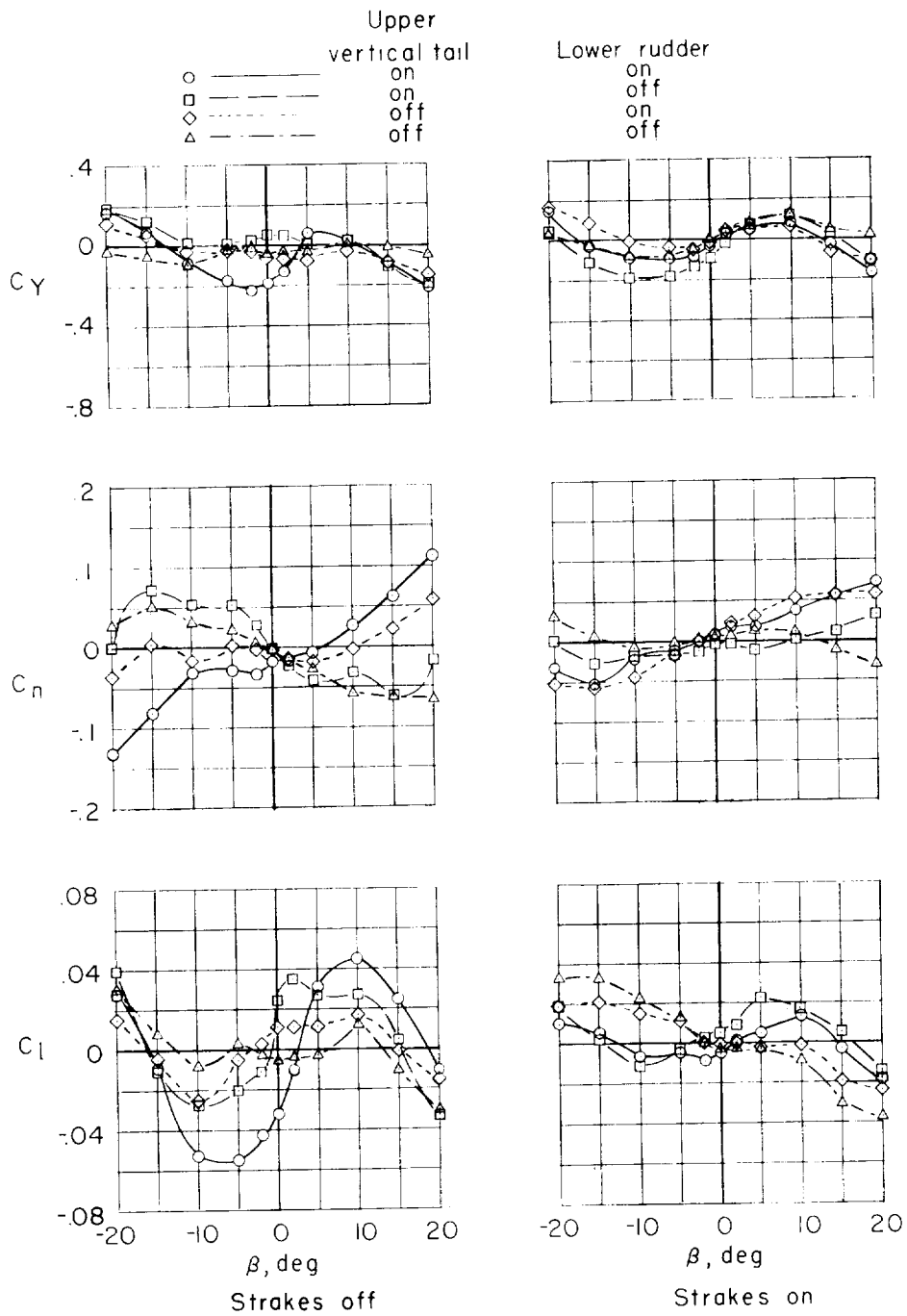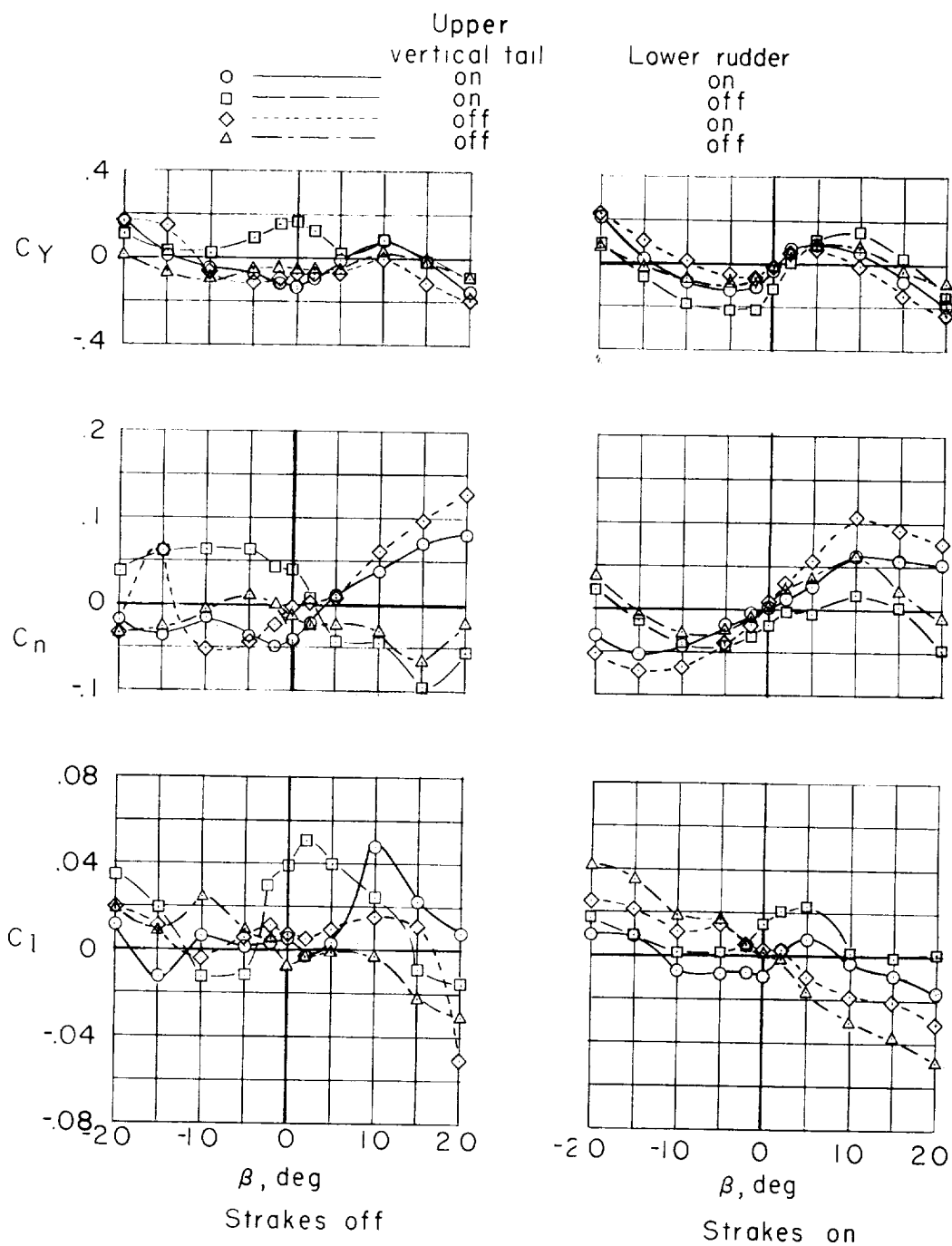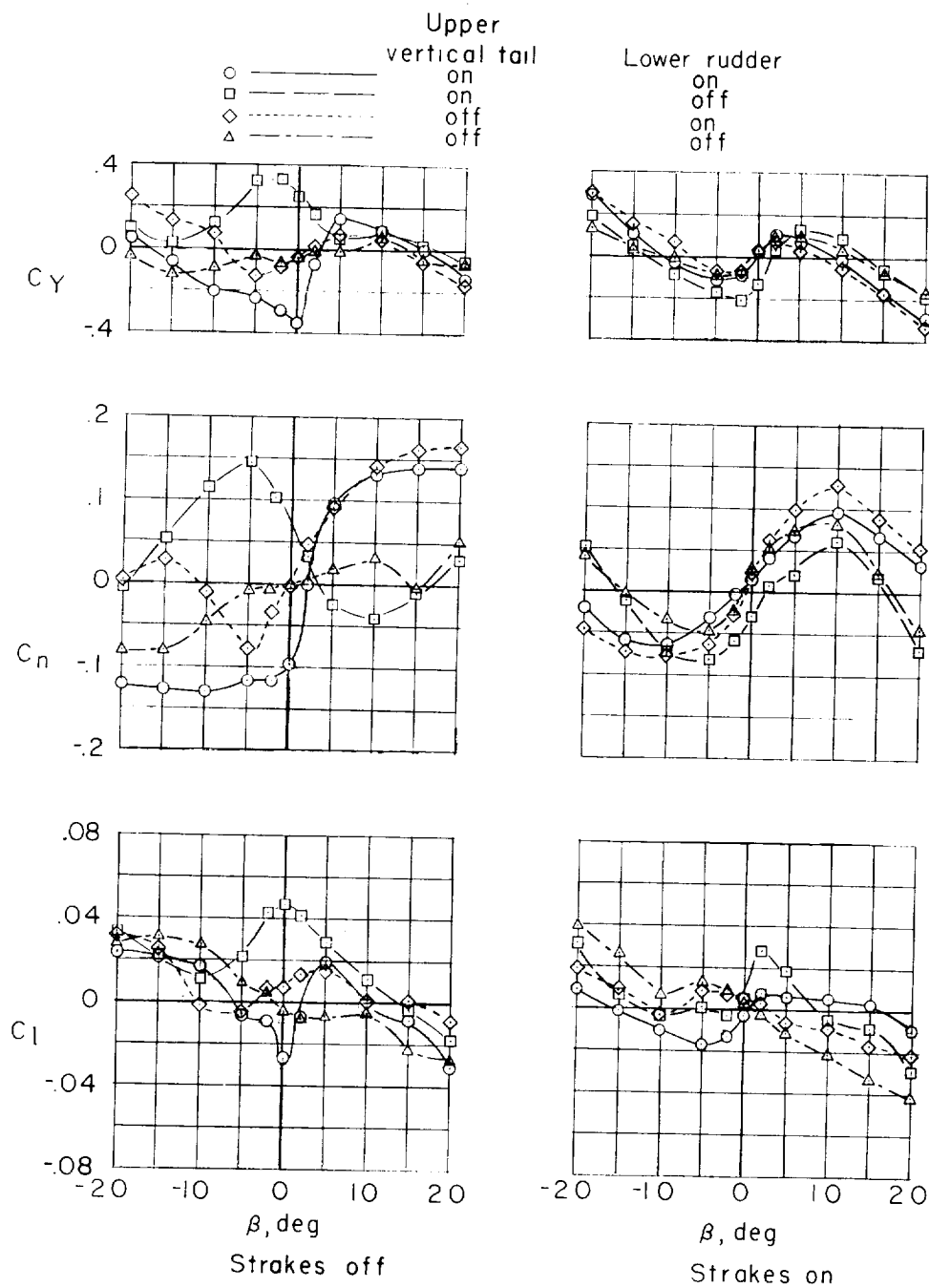
(g) α = 40°.

Figure 8.- Concluded.

38
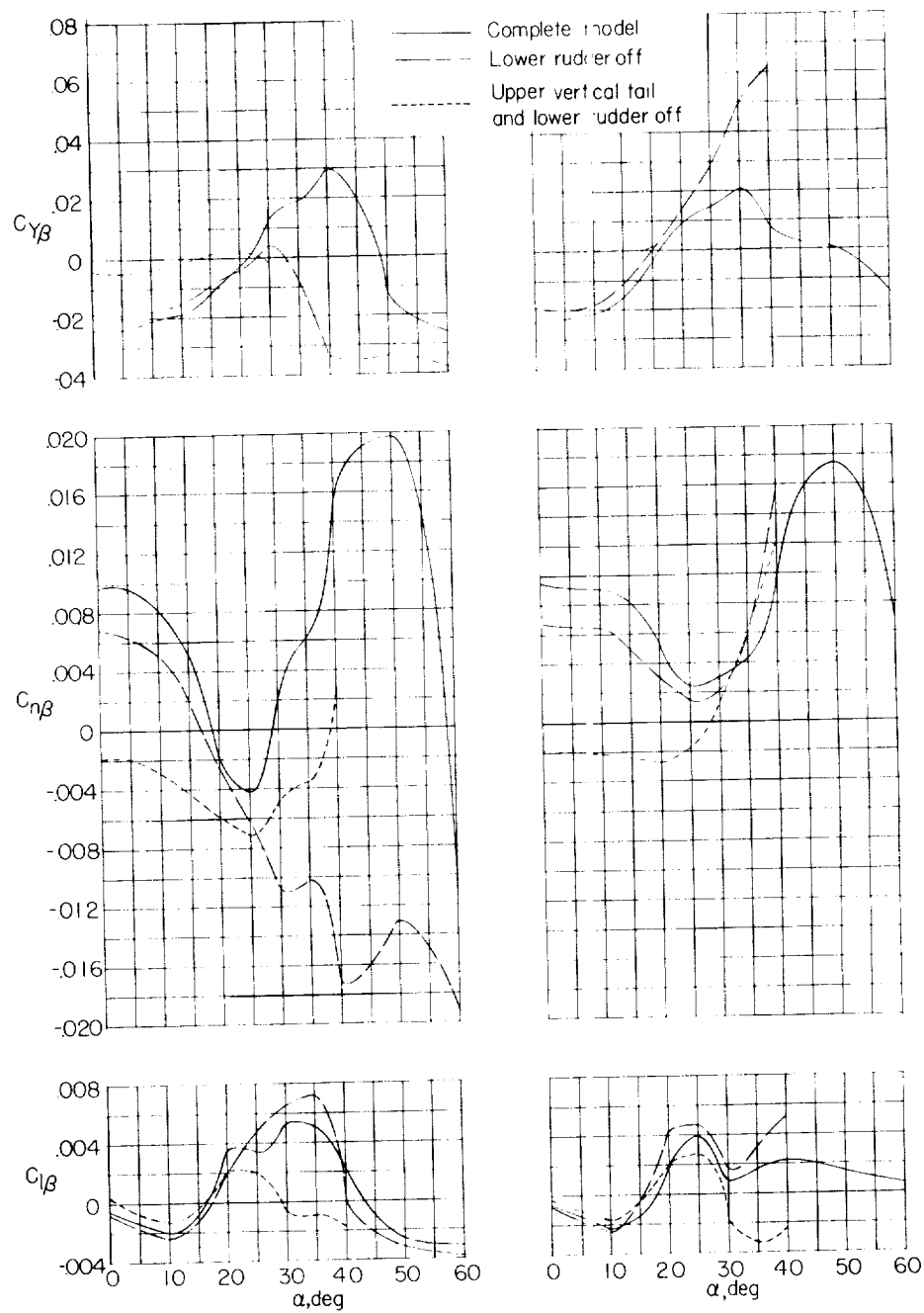
(a) Strakes off. (b) Strakes on.

Figure 9.- Variation of static sideslip derivatives with angle of attack for flight-test model. $\delta_h = 0^\circ$.
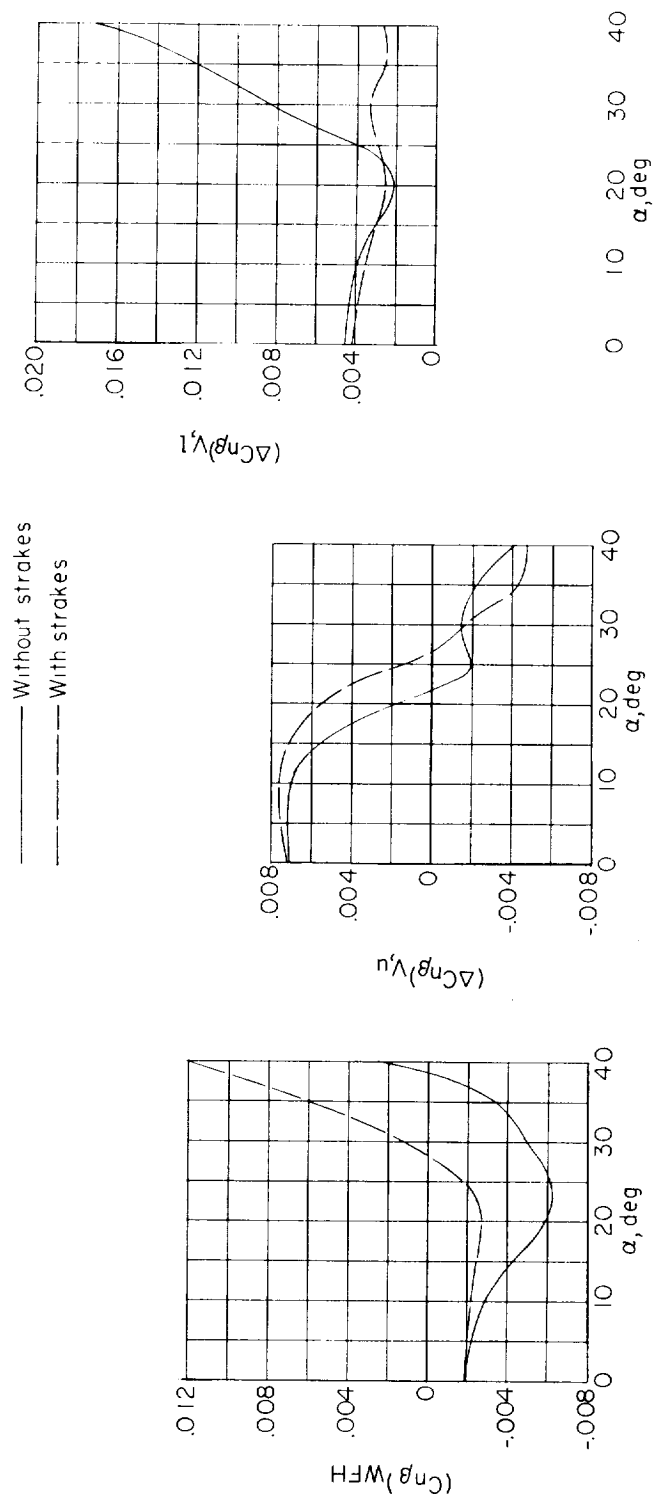
(a) Wing-fuselage-horizontal tail combination.

(b) Upper vertical-tail increment.

(c) Lower rudder increment.

Figure 10.- Effect of strakes on contribution of various model components to static directional stability. Flight-test configuration.
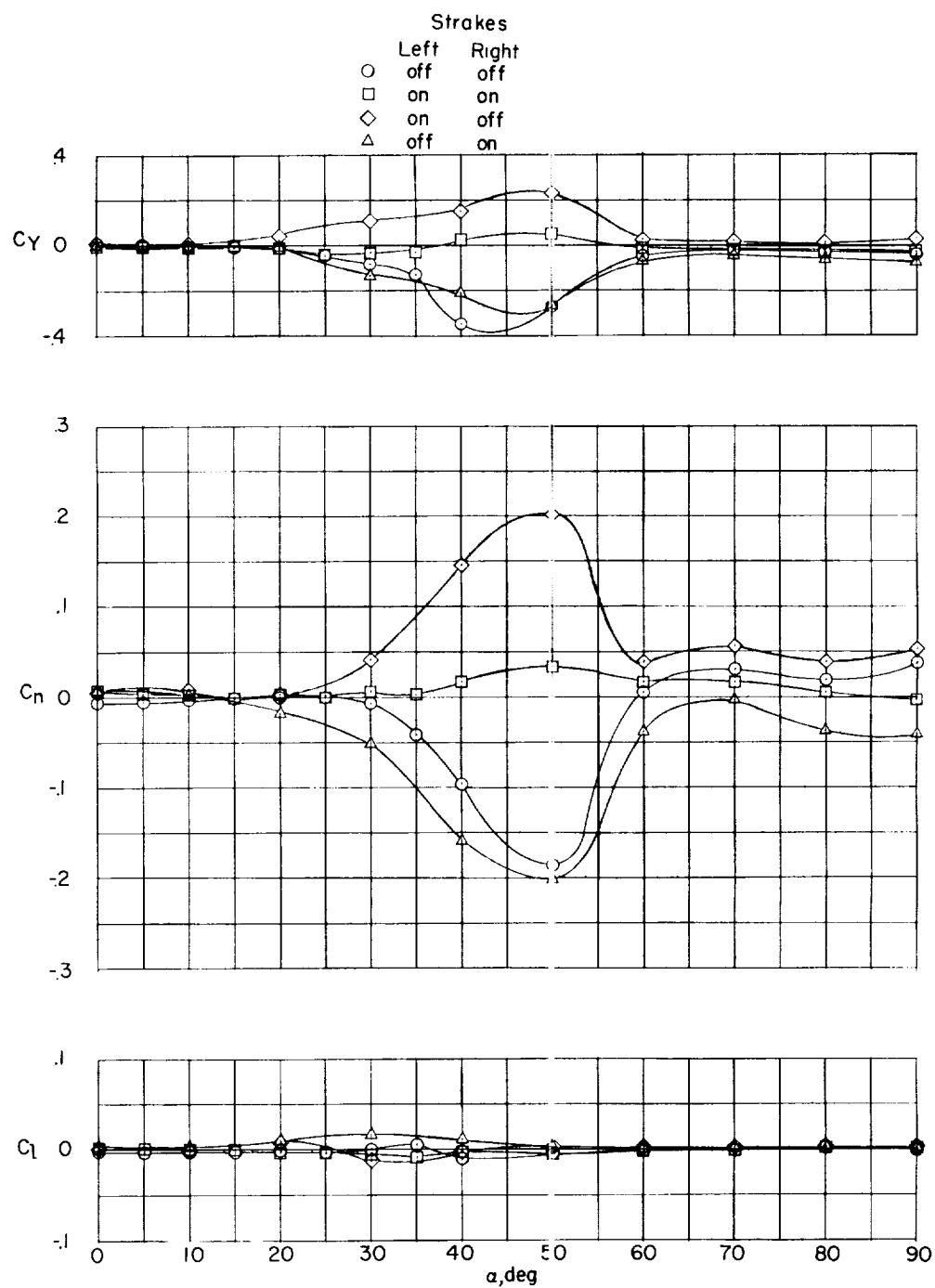
Figure 11.- Effect of strakes on variation of static lateral coefficients with angle of attack at zero sideslip. Flight-test configuration; $\delta_h = 0^\circ$.
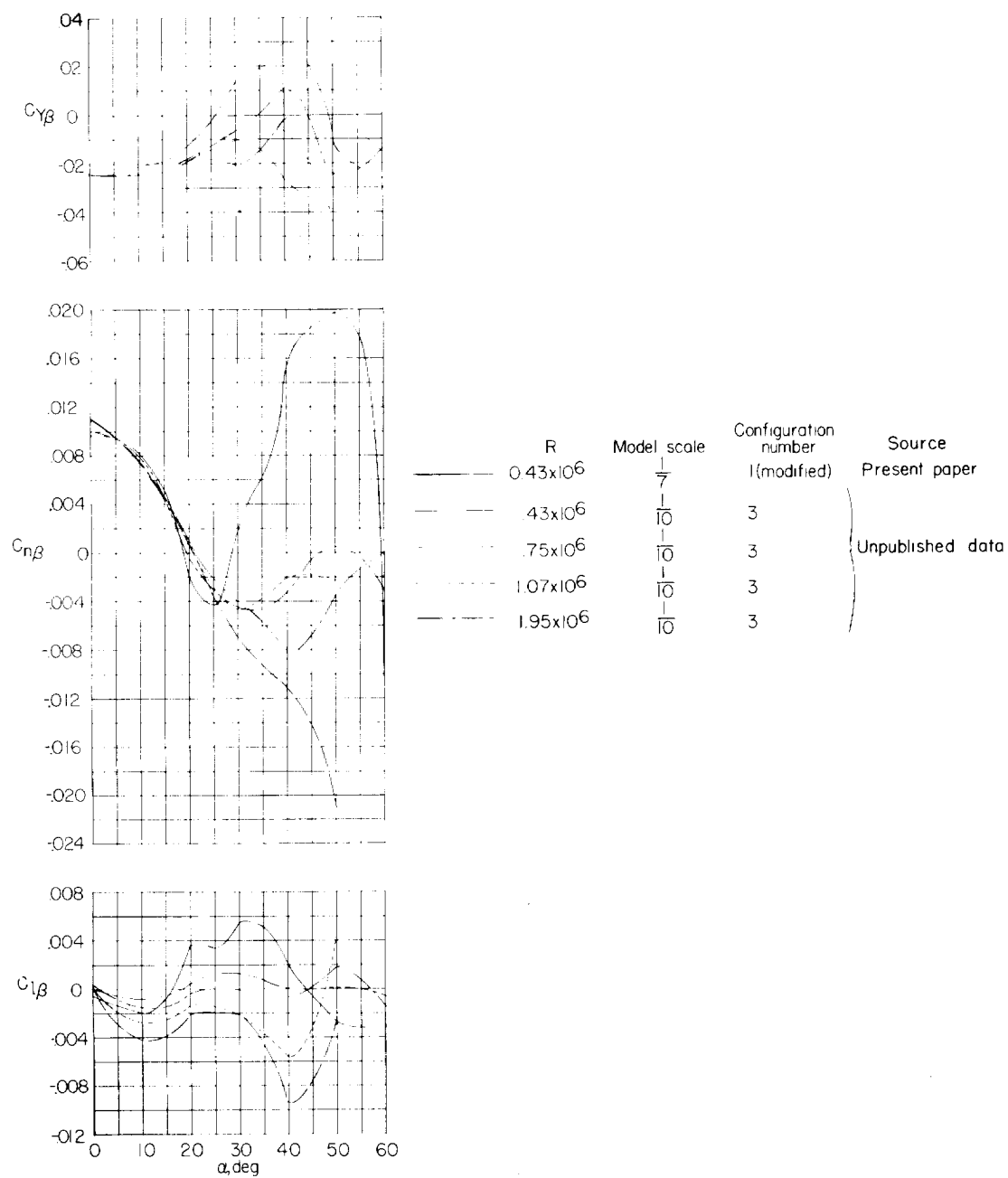
$C_{Y\beta}$

.04
.02
0
-.02
-.04
-.06

$C_{n\beta}$

.020
.016
.012
.008
.004
0
-.004
-.008
-.012
-.016
-.020
-.024

R	Model scale	Configuration number	Source
0.43x10^6	$\frac{1}{7}$	I(modified)	Present paper
.43x10^6	$\frac{1}{10}$	3	
.75x10^6	$\frac{1}{10}$	3	Unpublished data
1.07x10^6	$\frac{1}{10}$	3	
1.95x10^6	$\frac{1}{10}$	3	

$C_{l\beta}$

.008
.004
0
-.004
-.008
-.012

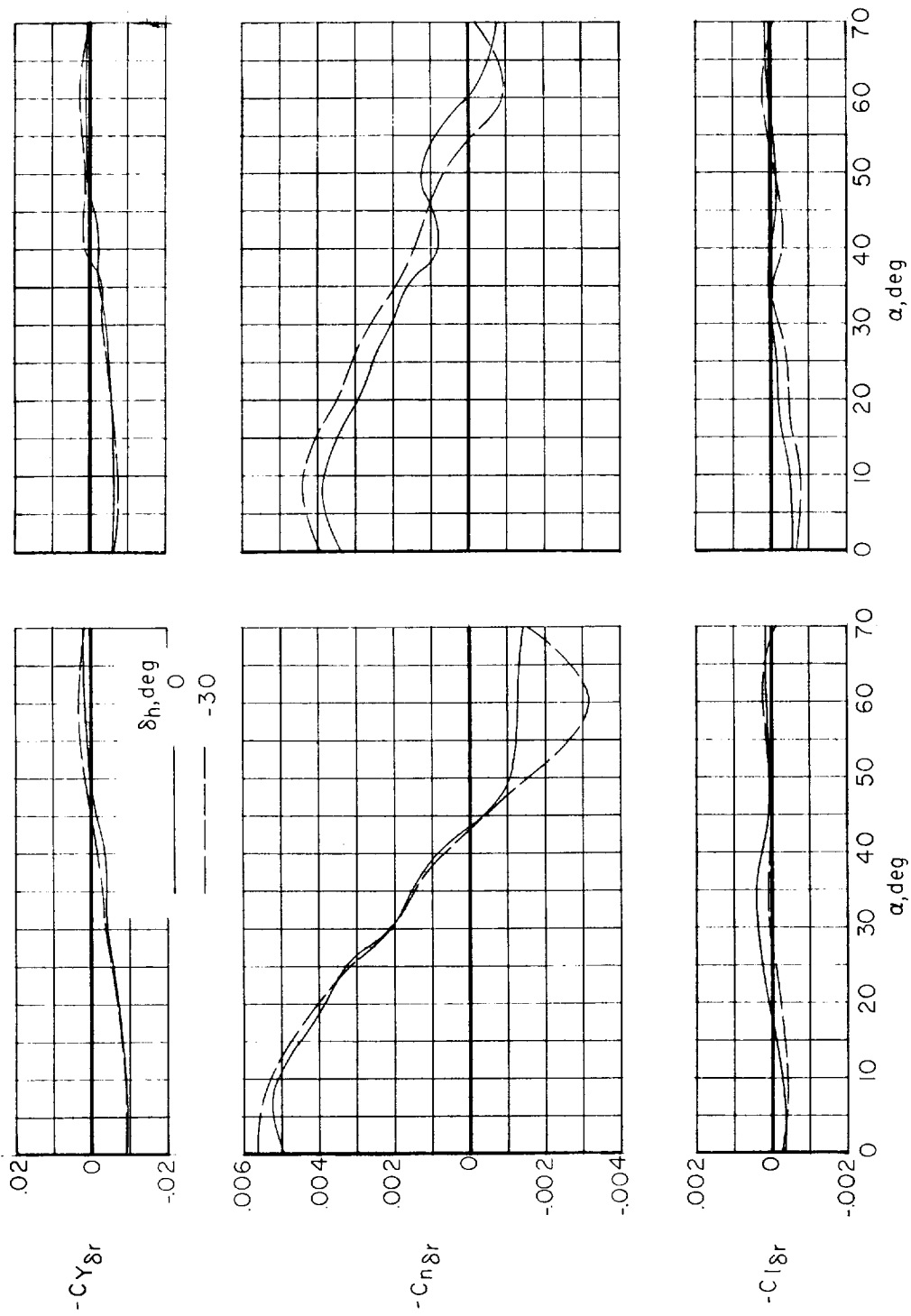0 10 20 30 40 50 60
α, deg

Figure 12.- Effect of model geometry and Reynolds number on variation of static sideslip derivatives with angle of attack (1/7-scale model, flight-test configuration; 1/10-scale model, configuration 3). Strakes off; $\delta_h = 0°$.

δ_h, deg
0
-10
-20
-30
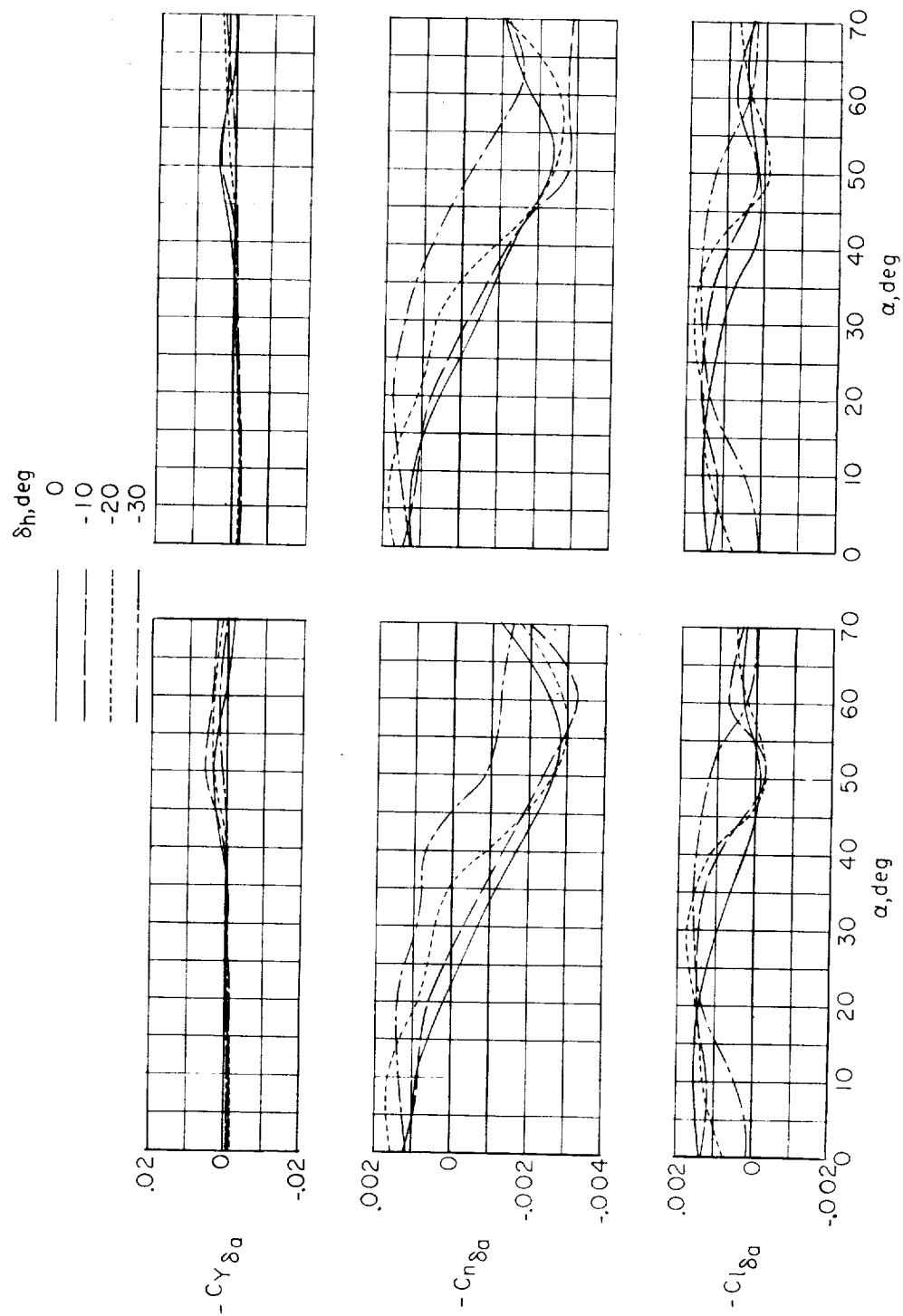
(a) Complete configuration.

(b) Lower rudder off.

Figure 13.- Roll-control effectiveness of 1/7-scale flight-test model. $\delta_r = 0°$; $\beta = 0°$

(a) Complete configuration.

(b) Lower rudder off.

Figure 14.- Rudder effectiveness of 1/7-scale flight-test model. $\delta_a = 0°$; $\beta = 0°$.

(a) Yawing-moment coefficients due to control.
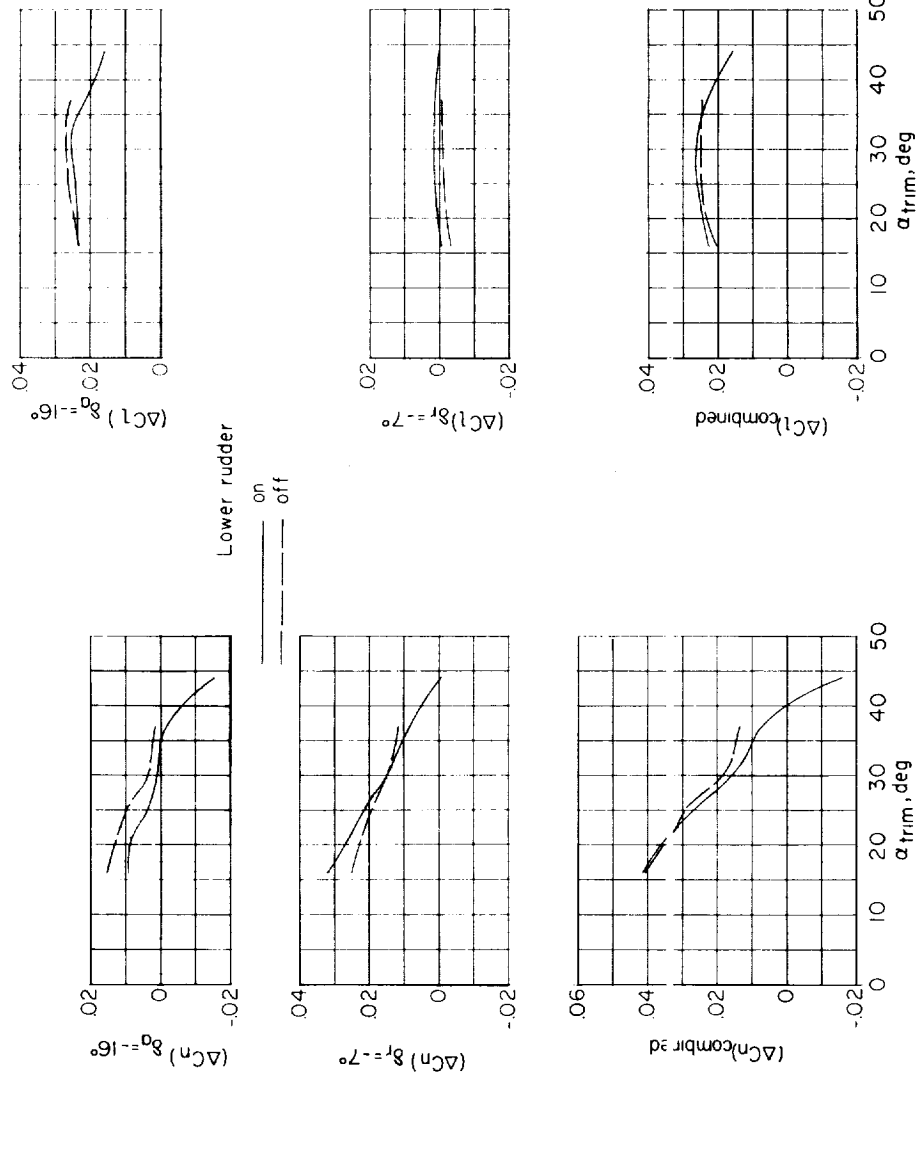
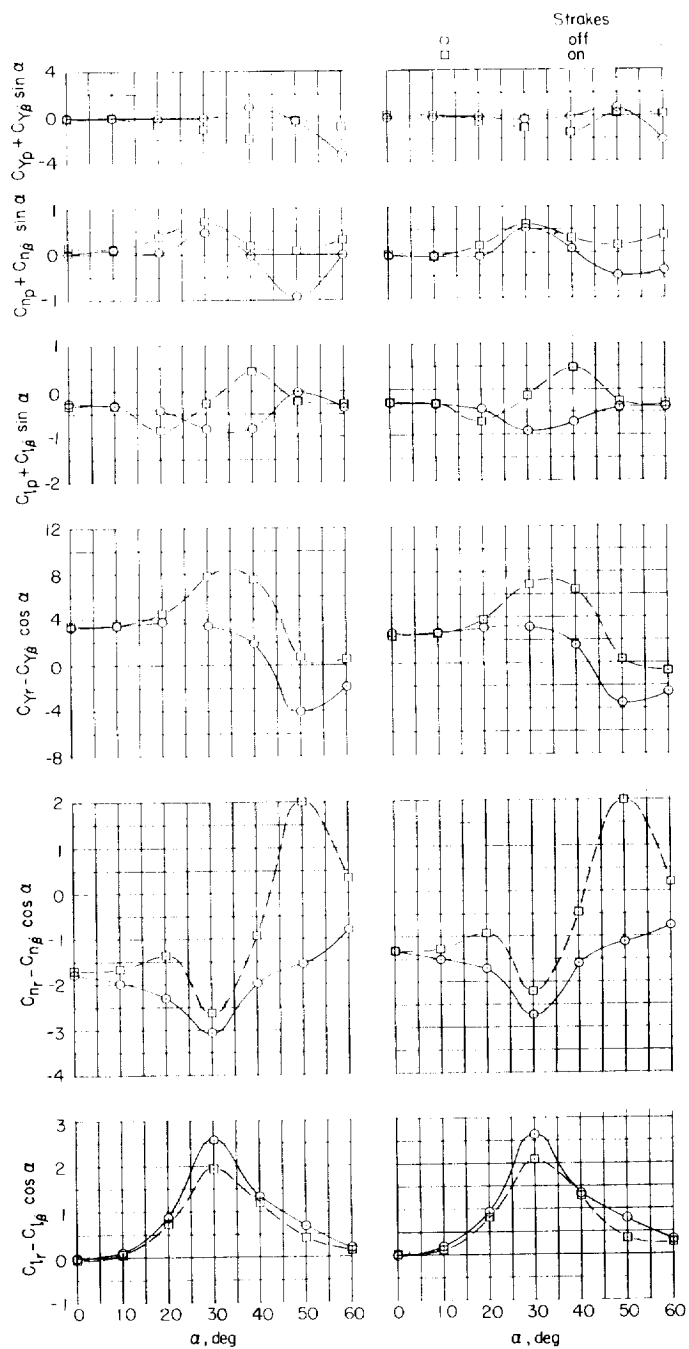(b) Rolling-moment coefficients due to control.

Figure 15.- Increments in yawing- and rolling-moment coefficients produced by control-surface deflections used in flight tests of 1/7-scale model for longitudinal trim conditions. (Right roll control and rudder deflections of -16° and -7°, respectively.) $\beta = 0°$.

(a) Complete configuration.   (b) Lower rudder off.

Figure 16.- Rotary oscillation derivatives of 1/7-scale flight-test model. $\delta_h = 0°$; $k = 0.10$.